# Salt Water Modeling of Fire Induced Flows in Multicompartment Enclosures



K.D. Steckler
H.R. Baum
J.G. Quintiere

U.S. DEPARTMENT OF COMMERCE
National Bureau of Standards
National Engineering Laboratory
Center for Fire Research
Gaithersburg, MD 20899

March 1986



red in part by:
Taylor Naval Ship Research
Development Center
sda, MD

NBSIR 86-3327

# SALT WATER MODELING OF FIRE INDUCED FLOWS IN MULTICOMPARTMENT ENCLOSURES

K.D. Steckler
H.R. Baum
J.G. Quintiere

U.S. DEPARTMENT OF COMMERCE
National Bureau of Standards
National Engineering Laboratory
Center for Fire Research
Gaithersburg, MD 20899

March 1986

Sponsored in part by:
David Taylor Naval Ship Research
and Development Center
Bethesda, MD

U.S. DEPARTMENT OF COMMERCE, Malcolm Baldrige, *Secretary*
NATIONAL BUREAU OF STANDARDS, Ernest Ambler, *Director*

TABLE OF CONTENTS

LIST OF FIGURES

LIST OF FIGURES (continued)

NOMENCLATURE

| | |
|---|---|
| $c_p$ | specific heat of air |
| $\mathcal{D}$ | mass diffusivity of salt water in fresh water |
| F | ratio of salt water plume's initial momentum flux to buoyancy flux, Eq. (16) |
| G | ratio of length scales cubed, Eq. (15) |
| $\bar{g}$ | gravitational acceleration |
| H | full-scale enclosure height |
| h | reduced-scale enclosure (model) height |
| k | thermal conductivity of air |
| $\bar{k}$ | vertical unit vector; either upward or downward |
| L | characteristic length of heat source |
| $\ell$ | characteristic length of salt water source |
| $\dot{m}_o$ | mass release rate of salt |
| $\tilde{p}$ | pressure perturbation about hydrostatic pressure |
| P | Pr or Sc, Eq. (13) |
| Pr | Prandtl number for air, Eq. (13) |
| $\dot{Q}_o$ | heat release rate |
| Re | Reynolds number, Eq. (14) |
| Sc | Schmidt number for salt water in fresh water, Eq. (13) |
| T | temperature |
| $T_o$ | initial temperature |
| t | time |
| U | velocity scale, Eq. (11) |
| $\bar{u}$ | velocity |
| $v_o$ | velocity of salt water at source exit |
| $\bar{x}$ | position vector |

| | |
|---|---|
| $Y$ | salt mass fraction, $(\rho - \rho_o)/\rho_o$ |
| $z$ | distance from source measured along flow path |
| $z'$ | distance at which initial momentum effect becomes small |
| $z_d$ | height of interface between upper hot gas (salt water) layer and lower cool gas (fresh water) layer |
| $\zeta$ | density or temperature perturbation scale, Eq. (12) |
| $\rho$ | density |
| $\rho_o$ | initial density of fluid in enclosure |
| $\theta$ | nondimensional temperature, $(T - T_o)/T_o$, or mass fraction, Y |
| $\mu$ | viscosity of air or fresh water |

Superscripts

| | |
|---|---|
| * | nondimensionalized variable or operator, Eqs. (4-10) |
| ''' | per unit volume |

# SALT WATER MODELING OF FIRE INDUCED FLOWS IN MULTICOMPARTMENT ENCLOSURES

K.D. Steckler, H.R. Baum, and J.G. Quintiere

## Abstract

Salt water modeling is used to study fire-induced flows in multicompartment structures. Scaling laws relating salt water flows and hot gas flows are developed. Results from 1/20 scale salt water simulations of fire-induced flows in a single-story multiroom structure are shown to be in good agreement with available full-scale results. Experiments involving a 1/20 scale model of a U.S. Navy ship demonstrate the feasibility of using the technique to study hot gas flows in compartmented structures too complex to study economically by other means.

Key words: buoyant flow; corridors; flow visualization; salt water; scale models; scaling laws; smoke filling; smoke layers.

## 1. INTRODUCTION

A major threat to the safety of inhabitants of many multiroom and multistory structures containing a localized fire is the rapid flow of combustion products throughout the structure. The paths of these flows are often complex; for example, through a series of connecting doorways, halls, stairs, shafts, etc. The time-dependent position of the hot layer fronts, layer thicknesses, and concentrations are needed to assess the threat to life safety along these complex paths.

Several alternative approaches can be considered to elucidate and understand fire generated flows in complex structures. Full-scale experiments offer the most realistic approach, but they are expensive and difficult to instrument and analyze. Reduced-scale fire experiments can reduce cost, but present the same instrumentation problems as in full-scale. In principle, mathematical solution of the partial differential equations of fire and flow physics should enable the determination of fire phenomena in enclosures. But issues of turbulence modeling are not fully resolved and three-dimensional unsteady flow in complex geometries is still not practical using even the largest available computers. Less fundamental mathematical lumped-parameter or "zone" models [1] reduce the mathematical complexity of the multicompartment problem by treating the structure as a limited number of connected spatial zones. Their solution is amenable to common computers, but with no guarantee to their physical accuracy or completeness. Indeed, mixing between zones is only partially addressed, and no explicit attention is given to the time-dependent development of horizontal flows in large rooms and long corridors, and the development of vertical flows in tall shafts. One approach that physically models most of the flow characteristics and provides a clean environment for measurement with excellent flow visualization is the hydraulic analog technique known as salt water modeling. Moreover, this technique provides a relatively inexpensive approach for evaluating complex structures.

Salt water modeling substitutes turbulent buoyant salt water moving in fresh water for turbulent buoyant hot gas moving in cold gas. Since the driving phenomena for the two processes are identical -- buoyancy forces resulting from density differences -- the two processes can be related when viscous and heat transfer effects are small. Although this technique offers

great potential in fire modeling, it has neither been used much nor has it been well documented. Thomas et al. [2] used the salt water technique to show the effect of roof and side vents on clearing smoke from large rooms. Tangren et al. [3] applied the technique at 1/5 scale to study the densities and positions of hot gas layers produced by fires in a room with a doorway or window vent.

The current study was motivated by the desire to evaluate smoke movement in naval combat ships. The availability from the U.S. Navy of detailed 1/20 scale clear plastic ship models -- originally built for stress studies -- and large water tanks for laboratory testing presented a natural application for salt-water modeling. Moreover, a ship's structure contains many generic flow passages so as to make its study generally applicable. To establish a sound basis for use of the modeling technique in ship and other multiroom structures, a comparison was made between the salt-water analog and single-story full-scale multiroom fire experiment results. These salt water experiments were conducted at the same scale (1/20) as the ship model. Specifically, the time-dependent positions of the hot gas layers and their thicknesses were measured. These comparisons and a derivation of the governing equations with considerations needed to fulfill the requirements of the partial scaling relations will be presented. Finally, typical results from experiments conducted with a model of a U.S. Navy frigate will be presented.

## 2. ELEMENTS OF SALT WATER MODELING

Salt water modeling involves (1) formulating reasonably precise mathematical treatments of smoke and salt water flows, (2) choosing appro-

priate nondimensionalizing factors to reduce the two mathematical treatments to precisely the same form, (3) performing a salt water experiment in a scale model, taking care to insure that the salt water is injected so as to form a turbulent buoyancy-dominated plume, and (4) interpreting the salt water results in terms of full-scale smoke movement via the analysis that led to the reduced forms of the equations. These steps establish the salt water experiment as an analog computer for solving full-scale smoke flow problems.

## 3. MATHEMATICAL FORMULATION

The theoretical basis for the salt water technique entails consideration of the governing equations for hot gas and salt water flows, source conditions, boundary conditions, and attendant approximations. Approximations are made so as to establish the partial scaling relations on the scale of the enclosure height, not on the scale of the source. Indeed, it will be shown that salt water modeling does not apply on the scale of the source owing to inherent differences between fire and salt water source conditions. Nevertheless, the initial effects become small at some distance from the source and the analogy is quite good beyond this distance.

### 3.1 Governing Equations

Baum and Rehm [4,5] derived nondimensional governing equations for the flow of invisid thermally nonconducting gas within an enclosure heated by a source sufficiently weak for the Boussinesq approximation to be valid for the flow outside the source region. They expressed the nondimensional variables in terms of a length scale H, the enclosure height; a length scale L, the

spatial extent of the source, shown in Fig. 1a; a velocity scale U, defined below; and a density (or temperature) perturbation scale $\zeta$, also defined below, where U and $\zeta$ were chosen to make the convective and buoyancy terms in the momentum equation of the same order. These equations are shown below with appropriate viscous and heat conduction terms added to facilitate later discussion of Reynolds number, Re, considerations pertinent to the current study.

$$\nabla^* \cdot \bar{u}^* = 0 \tag{1}$$

$$\frac{D\bar{u}^*}{Dt^*} + \nabla^* \tilde{p}^* - \theta^* \bar{k} = (1/Re)\, \nabla^{*2}\, \bar{u}^* \tag{2}$$

$$\frac{D\theta^*}{Dt^*} = GQ^* + (1/ReP)\, \nabla^{*2}\, \theta^* \tag{3}$$

The symbols in these equations are defined by the left sides of the following scaling equations:

| hot gas | salt water | |
|---|---|---|
| $H\nabla = \nabla^*$ | $= h\nabla$ | (4) |
| $\bar{x}_g/H = \bar{x}^*$ | $= \bar{x}_s/h$ | (5) |
| $t_g U/H = t^*$ | $= t_s U/h$ | (6) |
| $\bar{u}/U = \bar{u}^*$ | $= \bar{u}/U$ | (7) |
| $\tilde{p}/\rho_o U^2 = \tilde{p}^*$ | $= \tilde{p}/\rho_o U^2$ | (8) |

| hot gas | | salt water | |
|---|---|---|---|
| $(T - T_o)/T_o\zeta = \theta^*$ | $= Y/\zeta$ | | (9) |
| $\dot{Q}'''/(\dot{Q}_o/L^3) = 1 = Q^*$ | $= 1 = \dot{m}'''/(\dot{m}_o/\ell^3)$ | | (10) |
| $(\dot{Q}_o g/\rho_o c_p T_o H) = U$ | $= (\dot{m}_o g/\rho_o h)$ | | (11) |
| $U^2/gH = \zeta$ | $= U^2/gh$ | | (12) |
| $\mu c_p/k = Pr = P$ | $= Sc = \mu/\rho_o \mathcal{D}$ | | (13) |
| $\rho_o UH/\mu = Re$ | $= \rho_o Uh/\mu$ | | (14) |
| $(H/L)^3 = G$ | $= (h/\ell)^3$ | | (15) |

Equations (1-3) represent conservation of mass, momentum, and energy, respectively, at a point $\bar{x}_g$ in the gas away from enclosure surfaces at time $t_g$. The gas at $\bar{x}_g$ with velocity $\bar{u}$, temperature T, specific heat $c_p$, thermal conductivity, k, and viscosity $\mu$ is driven by a volumetric heat source $\dot{Q}''' = \dot{Q}_o/L^3$, where $\dot{Q}_o$ is the heat release rate and L characterizes the region in which it is released. The pressure is considered to be the sum of the hydrostatic pressure, which is a function of the initial density $\rho_o$ (and therefore constant), and a pressure perturbation $\tilde{p}$. The magnitude of gravitational acceleration is denoted by g and the initial gas temperature by $T_o$. $\bar{k}$ is a unit vector in the upward direction. The nondimensional variables $\bar{x}^*$, $t^*$, and $\theta^*$, shown on the left sides of Eqs. (5), (6), and (9) are identical to those used by Heskestad [6] to analyze full-scale fire experiments [7] in which fire strength was varied within a given enclosure.

The mathematical description of salt water flow in fresh water is formulated in a similar fashion. Figure 1b shows an inverted reduced-scale geometrically similar model of the enclosure mentioned in the above formulation of the gas flow equations. The reduced-scale model has a height h and is initially filled with fresh water. It contains a salt water source at coordinates scaled to correspond to those of the full-scale heat source. For a salt water source with spatial extent $\ell$, the governing equations for the flow of weakly buoyant salt water in fresh water can be nondimensionalized, in the manner described above, to the forms given by Eqs. (1-3). The symbols in these equations are now defined by the right sides of Eqs. (4-15). In this case, Eqs. (1-3) represent conservation of total mass, momentum, and salt mass, respectively, at a point $\bar{x}_s$ in the liquid away from the enclosure surfaces at time $t_s$. The liquid at point $\bar{x}_s$ with velocity $\bar{u}$, salt mass fraction Y, mass diffusivity $\mathcal{D}$, and viscosity $\mu$ is driven by a pressure perturbation $\tilde{p}$ caused by a volumetric salt water source $\dot{m}''' = \dot{m}_o/\ell^3$, where $\dot{m}_o$ is the mass release rate of salt and $\ell$ characterizes the region in which it is released. The density of fresh water is denoted by $\rho_o$ and $\bar{k}$ is a unit vector in the downward direction.

Since the nondimensional forms of the salt water and hot gas governing equations are identical, their solutions in terms of nondimensional variables are identical when G, Re, and P are preserved according to Eqs. (13-15). In practice, however, it is impossible to match these quantities in all cases. Nevertheless, inconsistencies can be minimized by careful selection of the salt water source conditions. The major requirement to keep in mind is that the salt water plume simulate the key features of a turbulent buoyant fire plume. Beyond this requirement, the specific gravity (density) and flow rate

of the salt water source are not critical. Indeed, the value of the scaling analysis is that the results from one salt water experiment can be used in Eqs. (5-12) to predict the results for other salt water source conditions or heat releae rates in geometrically similar enclosures.

### 3.2 Plume Reynolds Number

Turbulent fire plumes have Reynolds numbers, defined by Eq. (14), on the order of $10^5$. This value is sometimes difficult to match in reduced-scale salt water experiments due to the reduced length scale and source restrictions described below. Nevertheless, turbulent plumes exist for Reynolds numbers down to $\sim 10^4$. When the Reynolds number is this large or larger, the molecular transport terms in Eqs. (2) and (3) become negligible in relation to the other terms and inconsistencies between Prandtl number for air, Pr, and Schmidt number for salt water in fresh water, Sc, become unimportant. Therefore, when the Reynolds number or the salt water plume is $\sim 10^4$ or larger, Eqs. (1-3) are essentially identical for hot gas and salt water flows and dimensional variables, such as $\bar{x}_g$ and $\bar{x}_s$ or $t_g$ and $t_s$, are related through Eqs. (5-12).

### 3.3 Plume Momentum

In real fires the turbulent hot gas plume is usually purely buoyant, with virtually no initial momentum flux. In contrast, the salt water must be introduced with some initial momentum. Operationally, this requires a compromise; the salt water flow rate must be large enough to produce a turbulent plume (large Re) but small enough to insure that buoyancy effects dominate

initial momentum effects over a large portion of the plume height. Following Tangren et al. [3], the effect of initial momentum is assessed in the current study by considering the ratio F of initial momentum flux to buoyancy flux at height z "above" the source; that is,

$$F = \rho v_o^2/2 \left(\rho - \rho_o\right) gz \tag{16}$$

where $v_o$ is the velocity at the source exit and $\rho$ and $\rho_o$ are the density of salt water and fresh water, respectively. At some distance $z = z'$, the initial momentum effect becomes small and a purely buoyant plume is approximated beyond $z'$.

### 3.4 Plume Mass Flux

The mass flux in a fire plume is large compared to the mass issuing from the source. Therefore, care must be taken in the salt water experiment to insure that the source mass flow (salt plus water) is small compared to the mass flow in the plume at some distance from the source; for example, at the ceiling "above" a simulated pool fire. In the current study, a point source plume model [3] is used to estimate plume mass flow.

### 3.5 Source Geometry

Fire is a volumetric heat source with a constantly changing, poorly defined spatial extent. As it is impossible to release salt in a precisely scaled volume corresponding to the full-scale situation, the condition set forth in Eq. (15) cannot be met precisely. Nevertheless, this condition can

be partially met by considering L as the diameter of the full-scale fire and $\ell = (h/H)L$ as the diameter of the planar salt water source.

### 3.6 Boundary Conditions

The previous justification for disregarding viscous and heat transfer effects does not apply to regions near the enclosure boundaries. When the Reynolds number of the salt water flow does not match that of the hot gas flow, drag effects, which are a weak function of Re, are not precisely simulated. A more serious limitation, however, is the inability of the salt water experiment to simulate heat transfer -- by means of salt transfer -- at the boundary surfaces. Consequently, buoyancy is maintained for a longer period in the simulation than in the full-scale situation. Since buoyancy drives the flow, the salt water results are conservative in the sense that the speed and spatial extent of the salt water flow in a complex structure are somewhat greater than would exist in a real fire situation.

## 4. EXPERIMENTAL TECHNIQUE

Figure 2 shows an inverted scale model of the structure of interest initially filled with fresh water. The model contains a salt water source consisting of a short length of 1.9 cm I.D. pipe filled with glass beads. The lower end of the pipe is covered with a piece of cloth to keep the beads in place. The source is connected through a flowrator to an open tank of dyed salt water, which has a specific gravity of 1.07 (10 percent NaCl by weight), located above the model. An experiment consists of flowing the salt water through the source at an appropriate rate while video cameras equipped with time base generators record the resulting flow on video tape.

# 5. EXPERIMENTAL RESULTS AND DISCUSSION

## 5.1 Multiroom Single-Story Structure

A 1/20 scale inverted clear plastic model of the full-scale test facility shown in Fig. 3 was constructed for the salt water experiments. The reduced-scale model was equipped with removable partitions to alter the length of the corridor as shown in this figure. This choice of geometry allowed comparison of salt water results with hot gas results obtained earlier by Cooper et al. [7] in the full-scale structure. They used a methane diffusion burner located near the floor and at the center of the burn room. Separate tests were conducted with the burner operating at 25, 100, and 225 kW. Layer interface heights versus time results were reported for the locations designated by the letters in Fig. 3. They defined the interface height as the height at which the temperature increase above ambient temperature was 10 percent of the temperature increase measured near the ceiling. These heights and times were then nondimensionalized according to the left sides of Eqs. (5) and (6). Typical results are shown as open symbols in Figs. 4 to 7. An equivalent scaling analysis of these full-scale data has been presented by Heskestad [6].

The 1/20 scale model was initially filled with fresh water to the level of a scaled vent which corresponded to the small slot vent at the floor of the full-scale facility. This vent maintained the liquid at the initial level throughout the experiment. The height of each compartment was 12.7 cm. The salt water source was mounted over the center of the "burn room" with its cloth-covered end facing downward and positioned just below the surface of the water. Since each of the full-scale experiments was conducted with a constant

fuel supply rate, the salt water was introduced at a constant flow rate and the subsequent flow throughout the model recorded on video tape. Typical flow patterns are shown in Fig. 8. The layer interface height versus time data at the locations identified by letters in Fig. 3 were taken from the video tape and nondimensionalized according to the right sides of Eqs. (5) and (6).

Source effects were evaluated in a preliminary series of experiments involving source flow rates in the range 20 to 60 ml(solutions)/s. Rates in the range 40 to 60 ml/s produced the best agreement with the full-scale results. At the center of this range, 50 ml/s, the Reynolds number is 9500, and from Eq. (16), $F = 1.0$ at $z = 0.19\ h$, and $F = 0.19$ at $z = h$. Therefore the plume is turbulent and buoyancy flux exceeds initial momentum flux over 80 percent of the plume height. A calculation, based on point source plume theory [3], indicates that the buoyant mass flow rate in the plume at the ceiling is four times the source flow rate. Consequently, the 50 ml/s flow rate produces a reasonable approximation to a purely buoyant plume over the height of the compartment $h = 0.127$ m. Flow rates below 40 ml/s tended to be too laminar to produce a good simulation of a fire plume. Consequently, all subsequent experiments were conducted at ~ 50 ml(solutions)/s (~5 g(salt)/s).

Typical salt water results are displayed as solid symbols in Figs. 4 to 7. Each figure demonstrates the ability of a single 1/20 scale salt water experiment to predict full-scale results in a geometrically similar enclosure for a range of fire strengths. Similar agreements between salt water and full-scale results for positions A and D are shown in Appendix A.

## 5.2 Multicompartment Multideck Ship

Since the 1/20 scale model of the Navy FFG-7 class frigate included numerous vents to the outside, experiments were conducted with the inverted model submerged in a large tank of fresh water. The heights of the smaller compartments in the ship were ~ 13 cm. Salt water sources were installed at two locations; one in a crew quarters located in the lower mid-section of the ship, and the other in a machinery space at the same level but located closer to the stern. All hatches, interior and exterior, were fully open.

Salt water was supplied to one of the sources at a constant rate of 50 ml/s and the subsequent flow throughout the ship was recorded on video tape. Figure 9 shows an inverted photograph of the ship approximately 450 s after activating the source in the crew quarters. The dyed salt water has spread through a large portion of the deck house and to the outside through exterior vents. Below the main deck, the flow is confined to the space between watertight bulkheads.

Equations (5) and (6) allow the results in Fig. 9 to be interpreted in terms of full-scale hot gas flows. The expression for $t^*$ relates the experimental time $t_s$ and mass flow of salt $\dot{m}_o$ to full-scale time $t_g$ and heat release rate $\dot{Q}_o$. For example, the conditions shown in Fig. 9 at $t_s$ = 450 s represent full-scale conditions at $t_g$ = 450 s when the full-scale heat release rate is 225 kW. Times to reach the same conditions at other heat release rates are easily calculated via the expression for $t^*$, Eq. (6). Additional photographs of the ship experiments are presented in Appendix B.

## 6. CONCLUSIONS

Scaling relations connecting reduced-scale salt water flows to full-scale hot gas flows have been developed. The scaling relations for position and time have been partially validated for four specific geometrical arrangements through comparisons of layer interface heights obtained in 1/20 scale salt water experiments and full-scale fire-induced flow experiments. Experiments involving a complex ship model have demonstrated the feasibility of using the salt water technique to investigate hot gas flows in structures too complex to study economically by other means.

## 7. ACKNOWLEDGMENTS

This work was sponsored in part by David Taylor Naval Ship Research and Development Center (DTNSRDC), Bethesda, MD under contract N00167-84WR4-0207. The authors would like to thank Messrs. W. Rinkinen and H. Wheelock of the National Bureau of Standards and Mr. G. Sikora of the DTNSRDC for their assistance with the experiments and data reduction.

## 8. REFERENCES

[1] Jones, W.W., Fire Safety Journal, 9, 55-59 (1985).

[2] Thomas, P.H., Hinkley, P.L., Theobald, C.R., and Simms, D.L., Investigations into the Flow of Hot Gases in Roof Venting, F.R. Technical Report No. 7, Dept. of Scientific and Industrial Research and Fire Offices' Committee Joint Fire Research Organization, London, 1963.

[3] Tangren, E.N., Sargent, W.S., and Zukoski, E.E., Hydraulic and Numerical Modeling of Room Fires, NSF Grant ENV 76-06660 and U.S. Dept. of Commerce, Nat. Bur. of Stand. Grant 5-9004, California Institute of Technology, Pasedena, CA, June 1978.

[4] Baum, H.R. and Rehm, R.G., Combustion Science and Technology, 40, 55-77 (1984).

[5] Rehm, R.G. and Baum, H.R., National Bureau of Standards Journal of Research, 83, 297 (1978).

[6] Heskestad, G., Physical Modeling of Smoke Movement, presented at ASTM E-5 Committee Meeting, Research Review Seminar on "Highlights of E-5's First 80 Years", Williamsburg, VA, December 9-14, 1984.

[7] Cooper, L.Y., Harkleroad, M., Quintiere, J., and Rinkinen, W., An Experimental Study of Upper Hot Layer Stratification in Full-Scale Multiroom Fire Scenarios, Paper 81-HT-9, 20th Joint ASME/AIChE National Heat Transfer Conference, Milwaukee, WI, August 2-5, 1981.

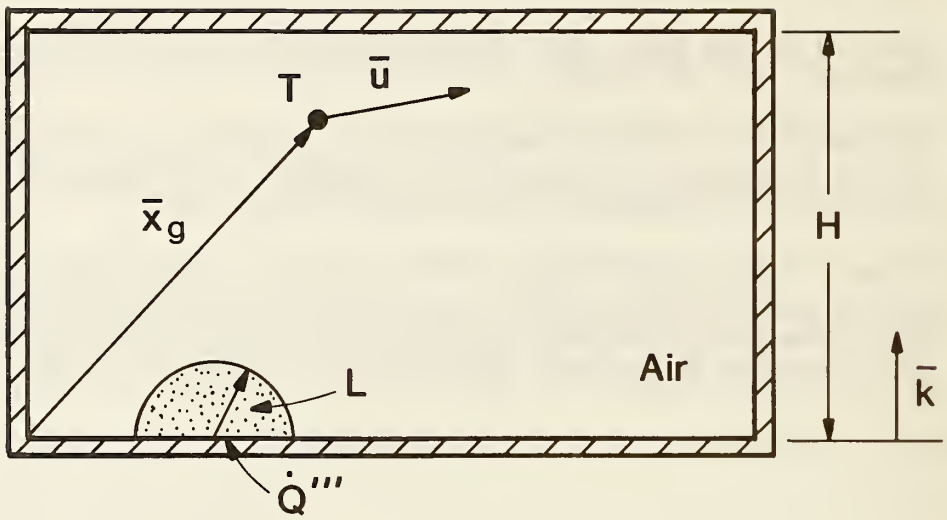


(a)

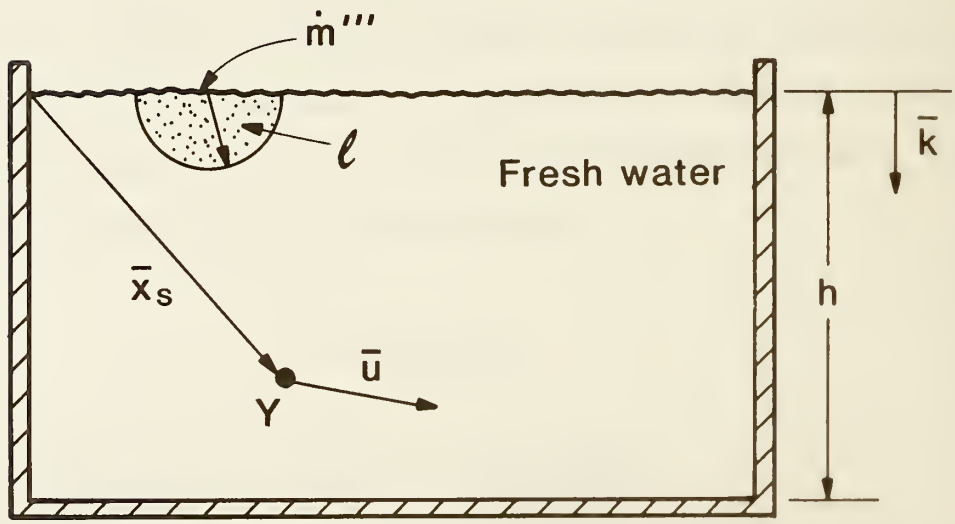


(b)

Fig. 1. Enclosures; (a) full-scale with heat source, (b) reduced-scale with salt water source.

# EXPERIMENTAL TECHNIQUE

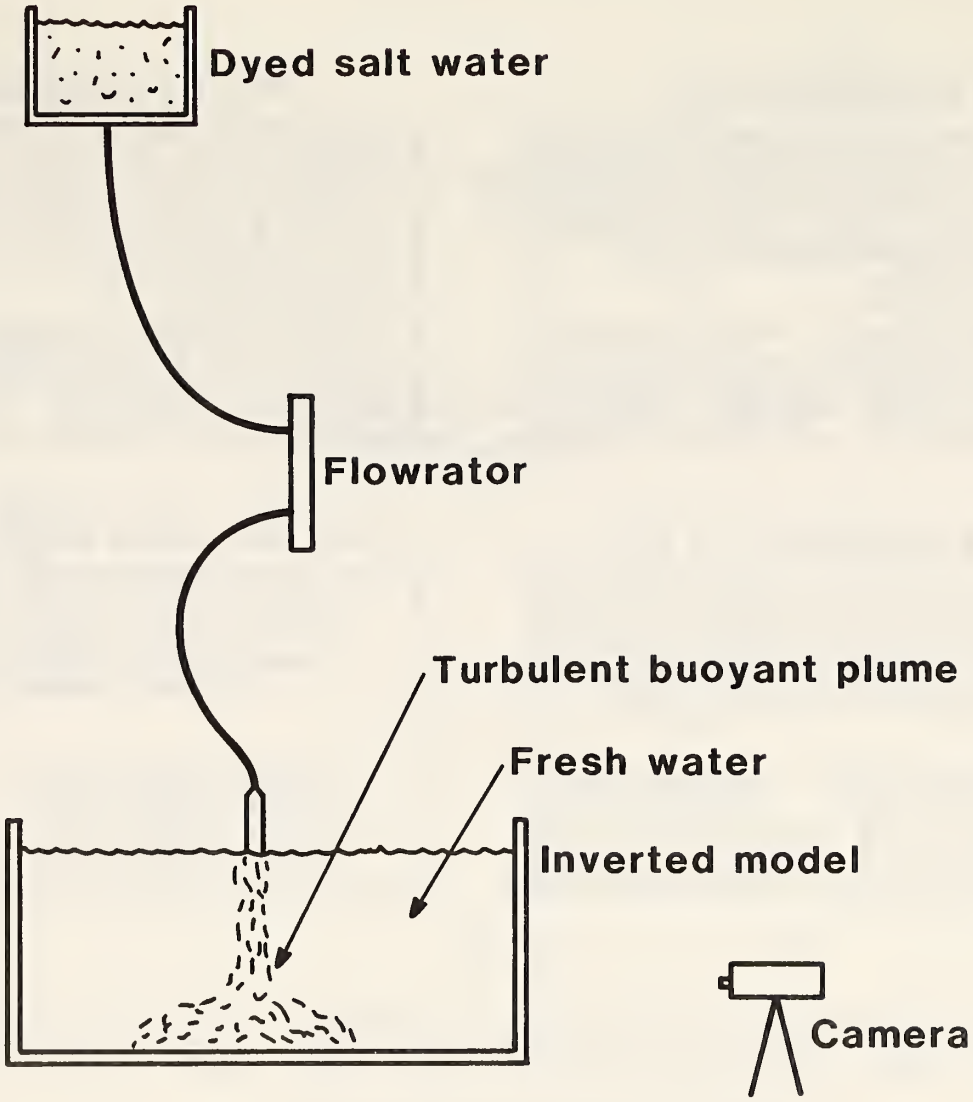


Fig. 2. Experimental arrangement.

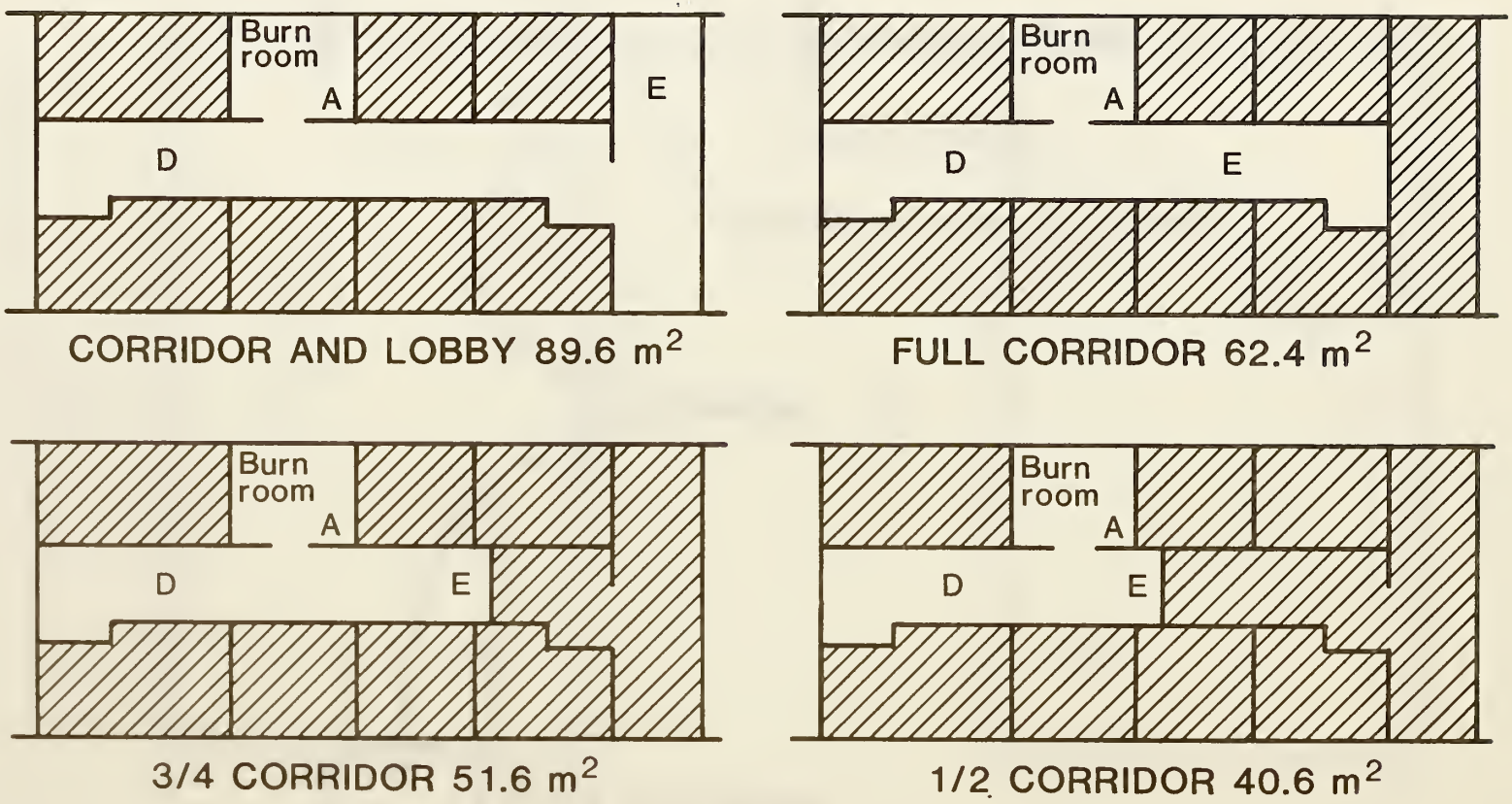


Fig. 3. Plan of full-scale test facility showing four test configurations.

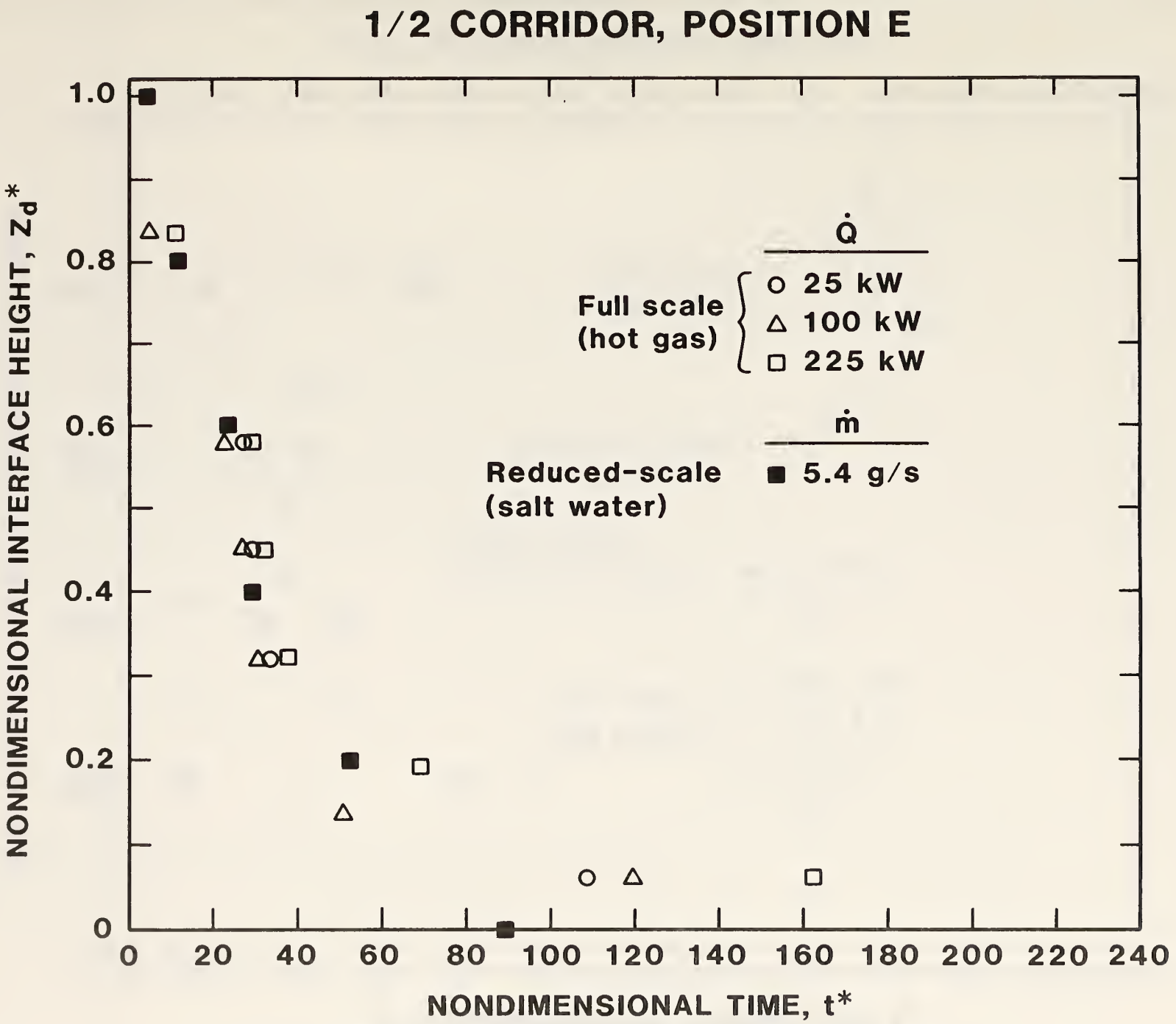


Fig. 4. Results for position E, 1/2 corridor configuration.

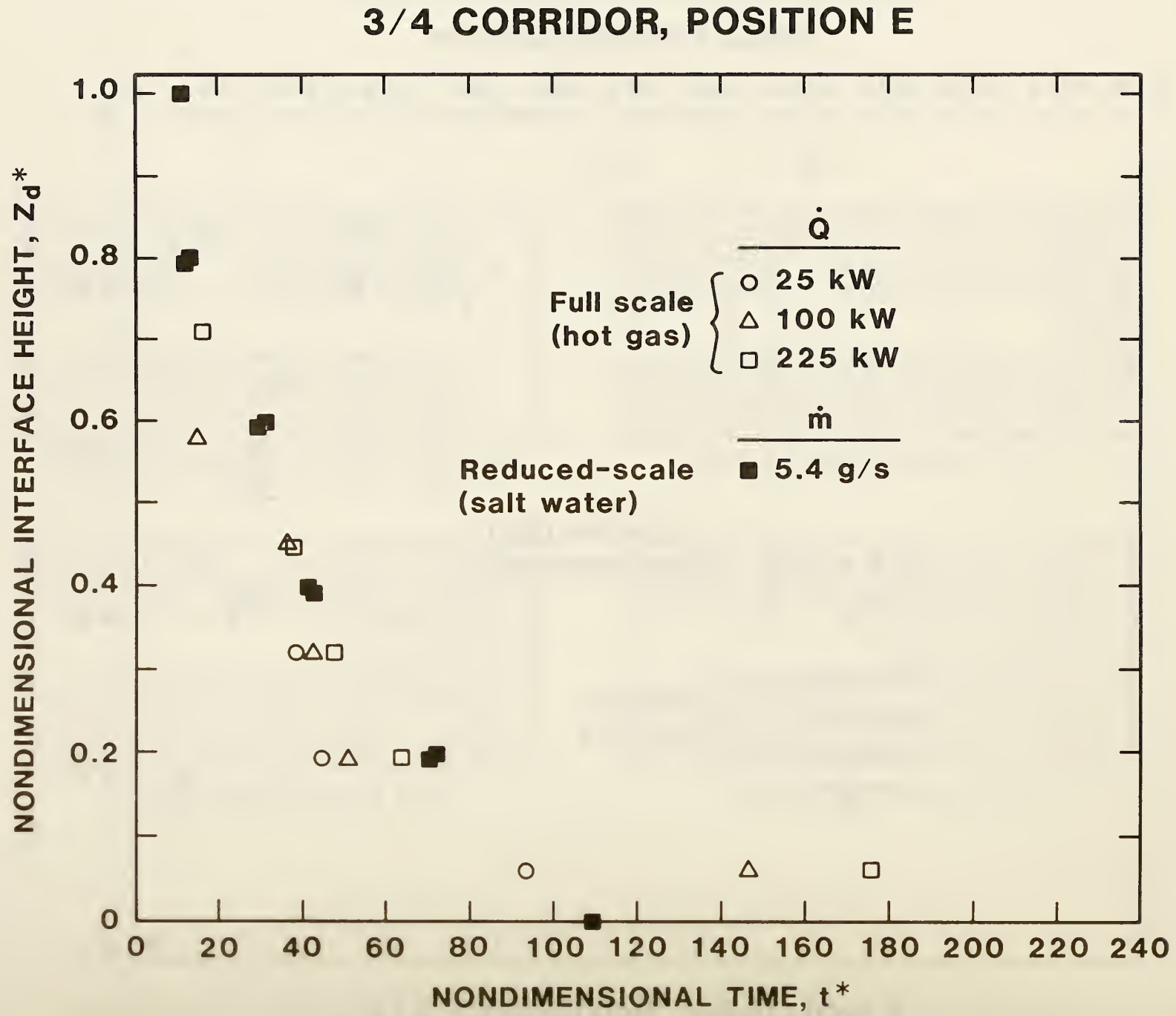


Fig. 5. Results for position E, 3/4 corridor configuration.

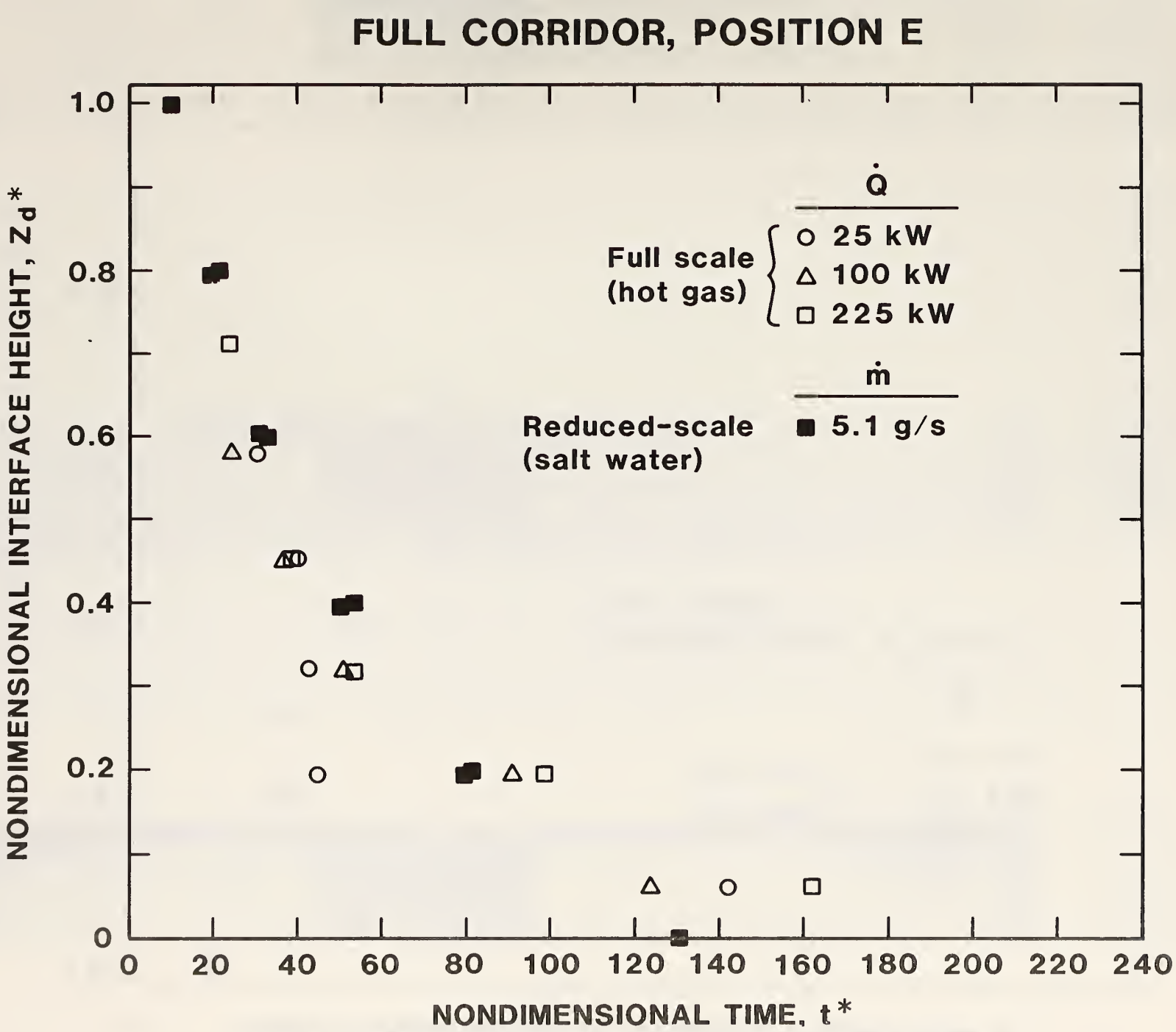


Fig. 6. Results for position E, full corridor configuration.

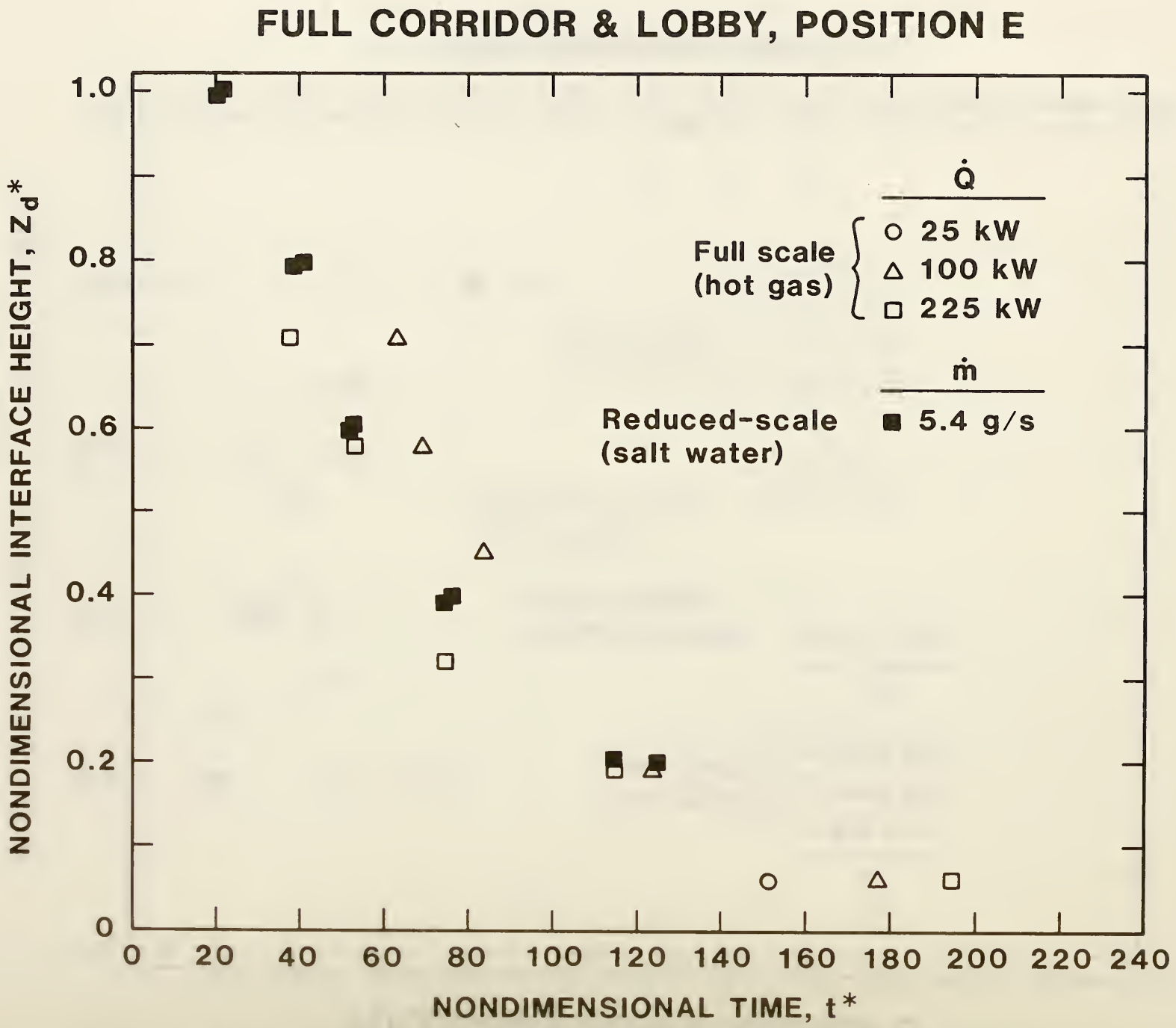


Fig. 7. Results for position E, full corridor plus lobby configuration.

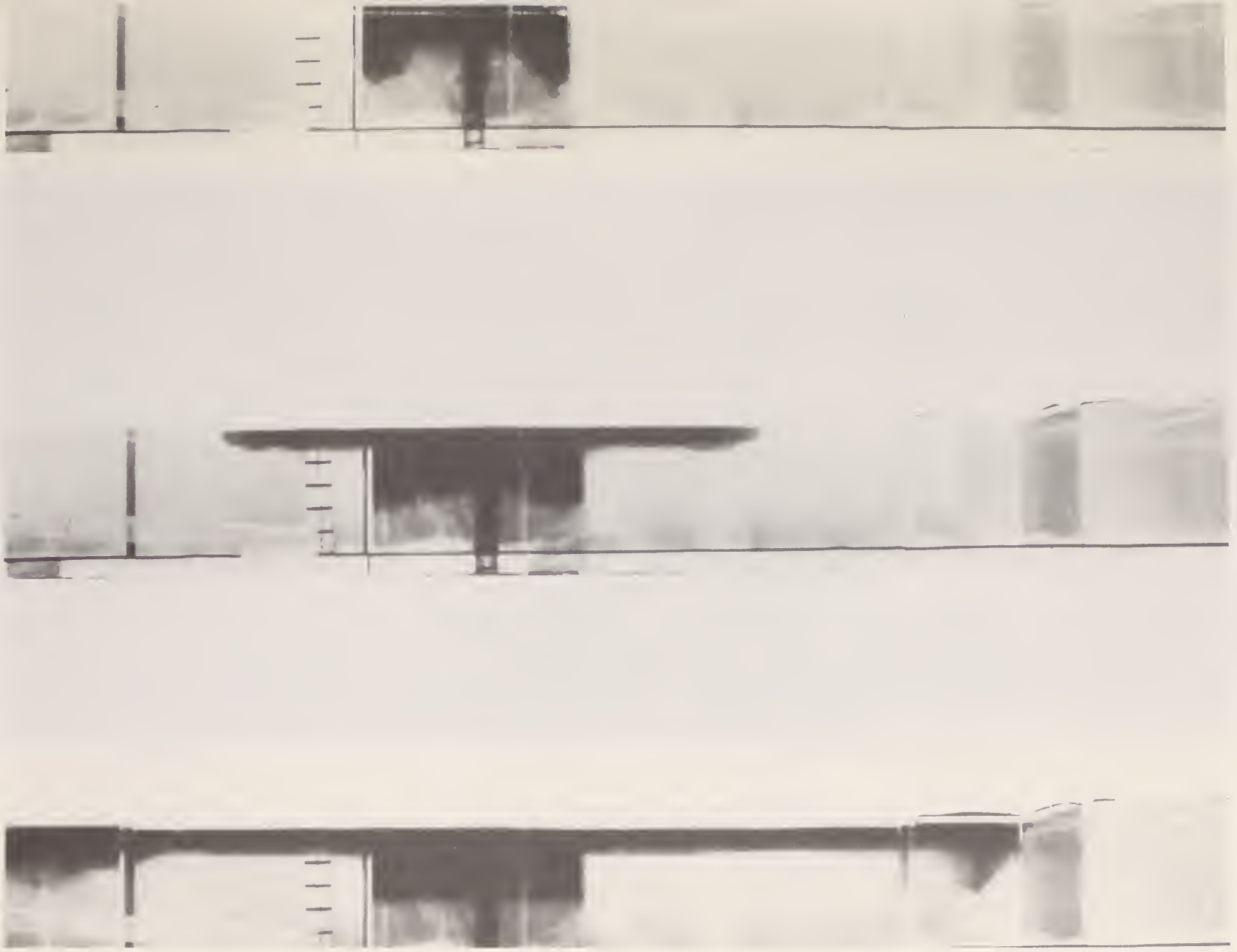

Fig. 8. Inverted photographs ($\bar{g}$ upward) of transient salt water flow in room and corridor. Lobby is on right.

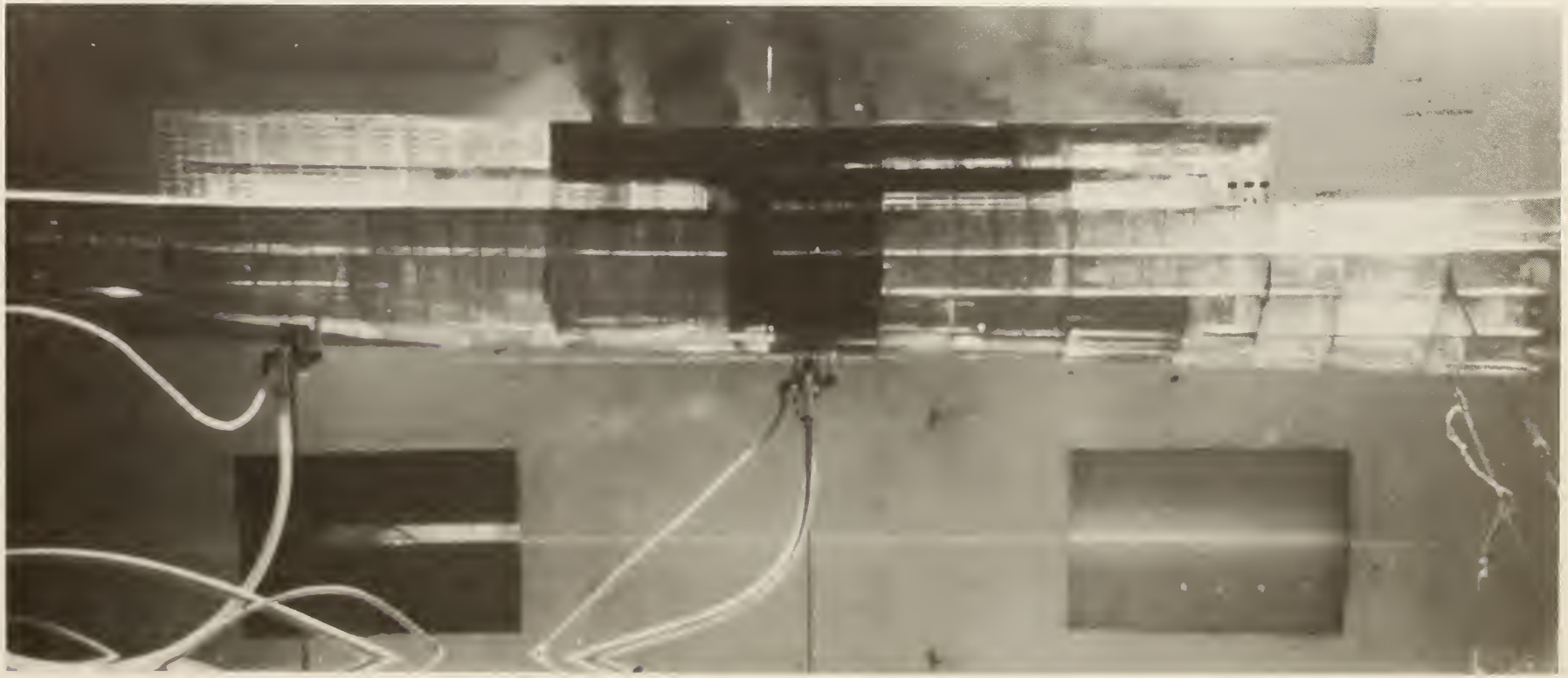

Fig. 9. Inverted photograph ($\bar{g}$ upward) of ship experiment approximately 450 s after activation of source. Bow is on right.

# APPENDIX A

Results for Positions A and D in Multiroom Single-Storey Structure

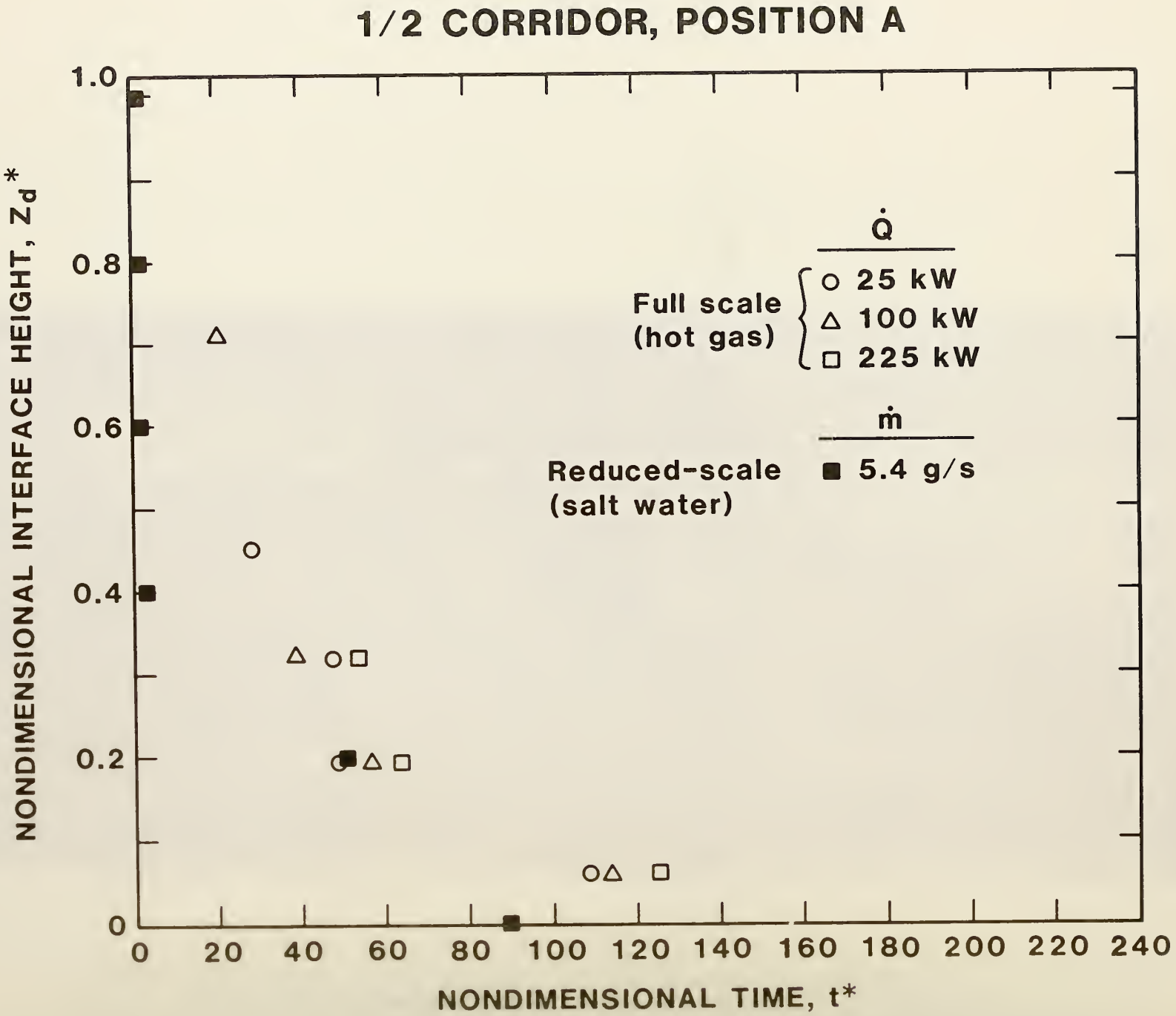


Fig. A-1. Results for position A, 1/2 corridor configuration.

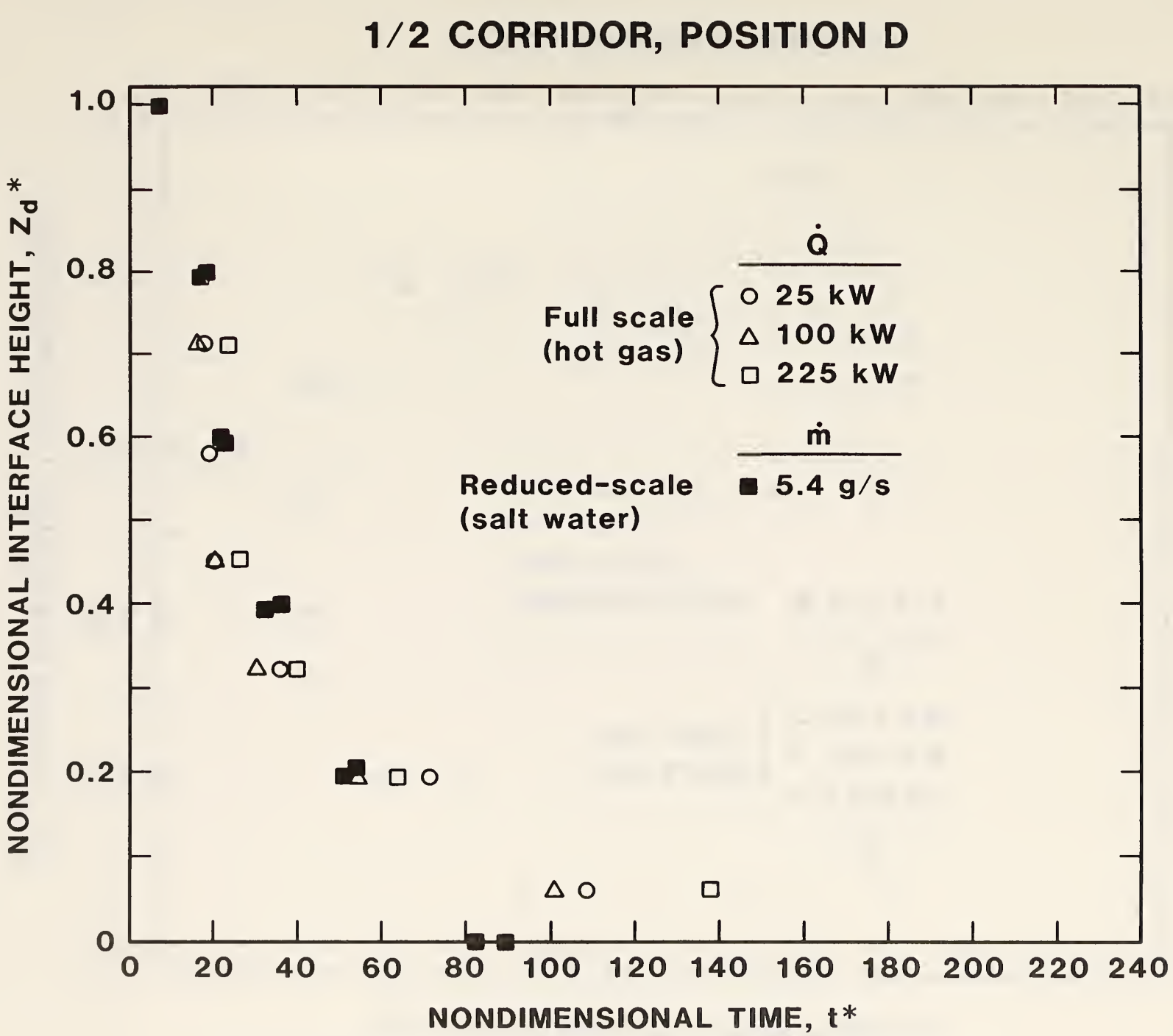


Fig. A-2. Results for position D, 1/2 corridor configuration.

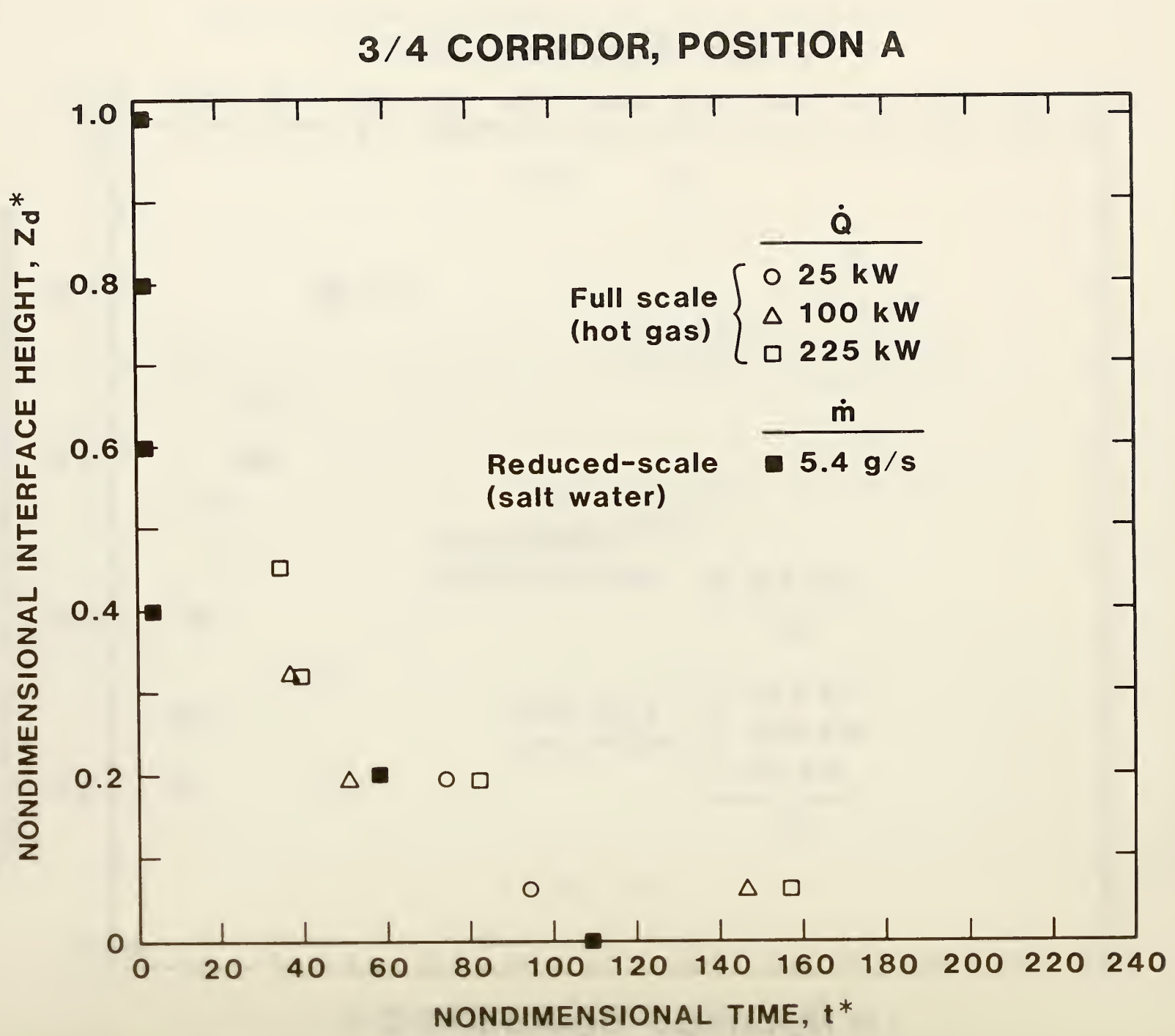


Fig. A-3. Results for position A, 3/4 corridor configuration.

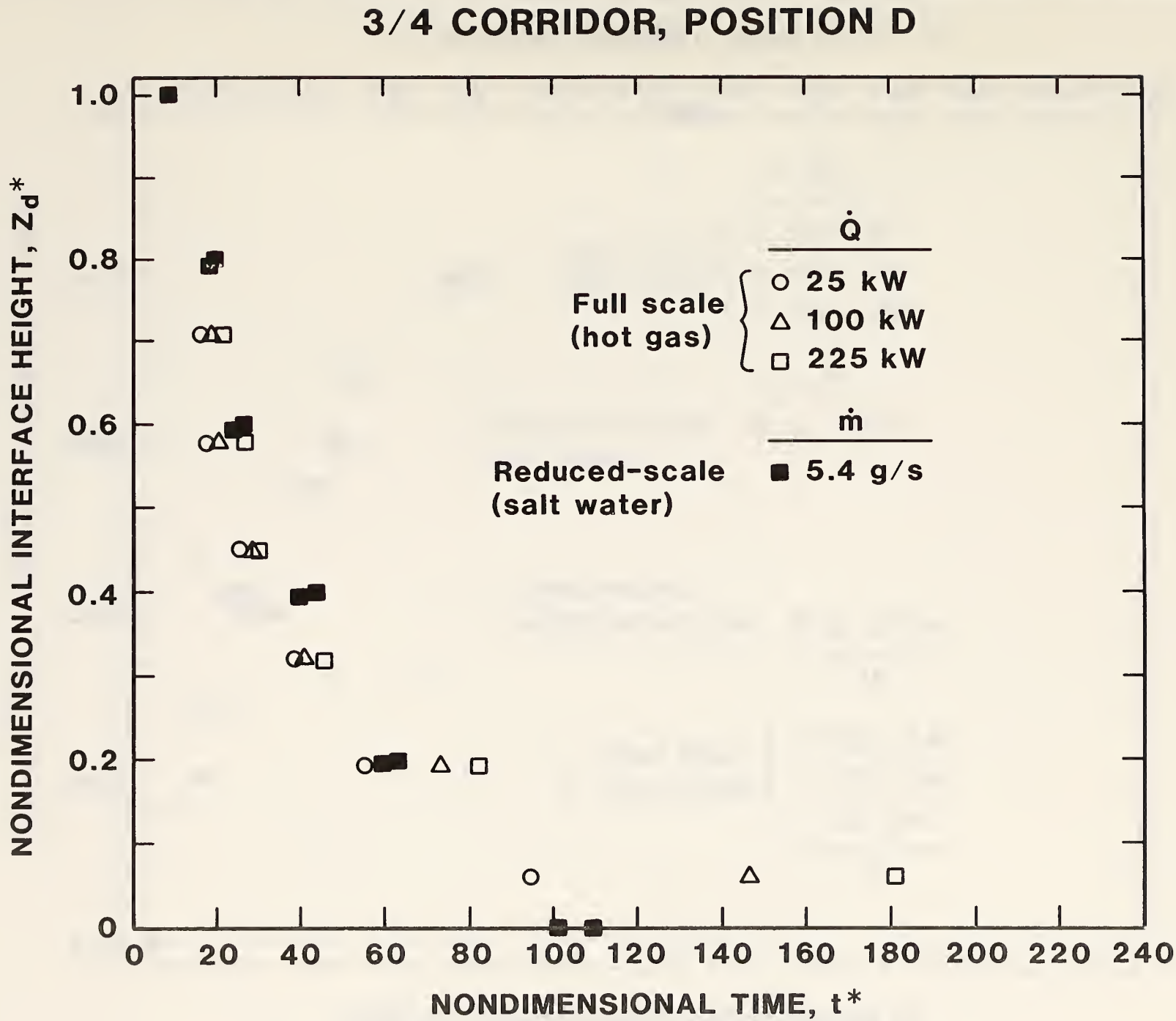


Fig. A-4. Results for position D, 3/4 corridor configuration

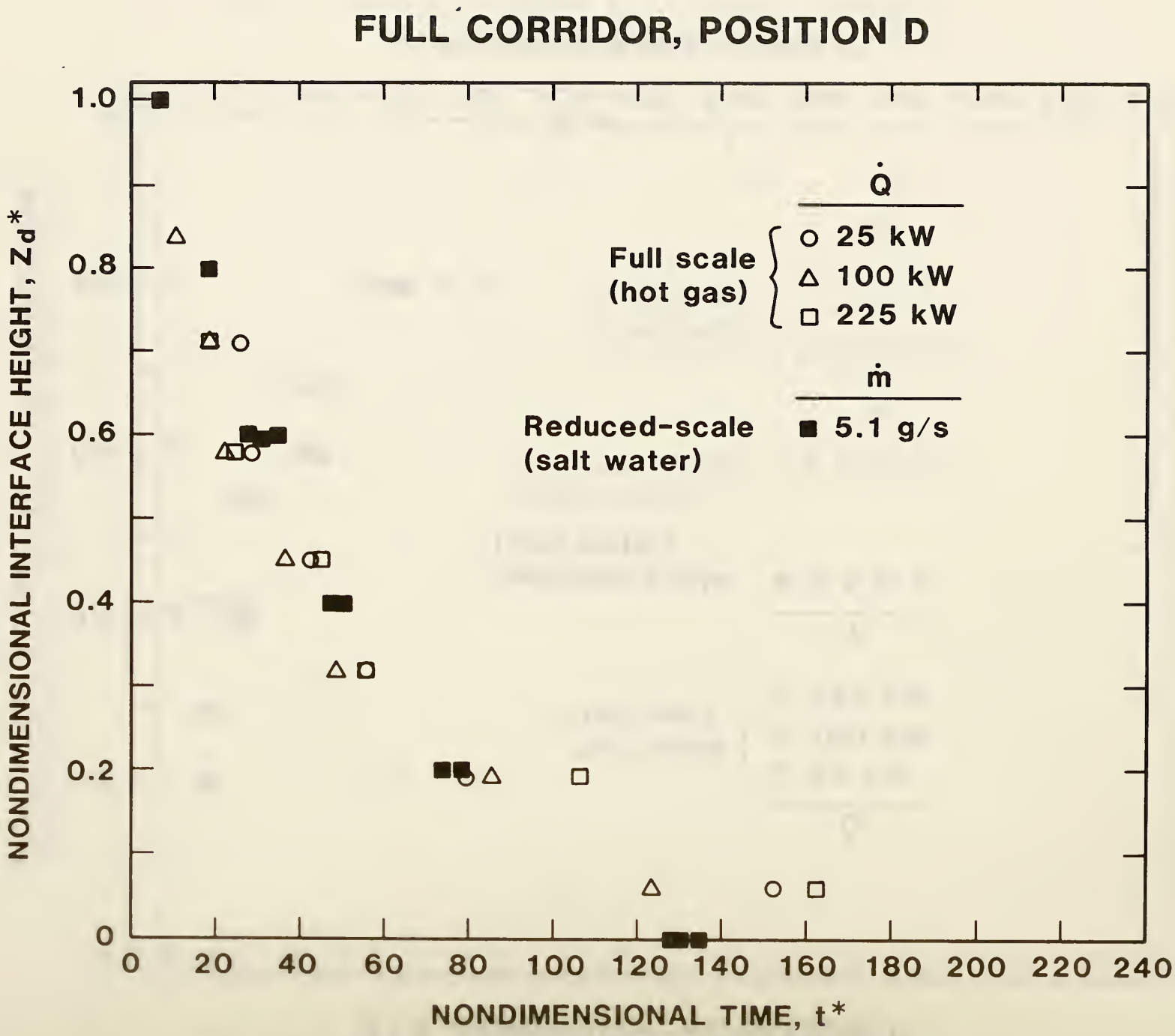


Fig. A-5. Results for position A, full corridor configuration.

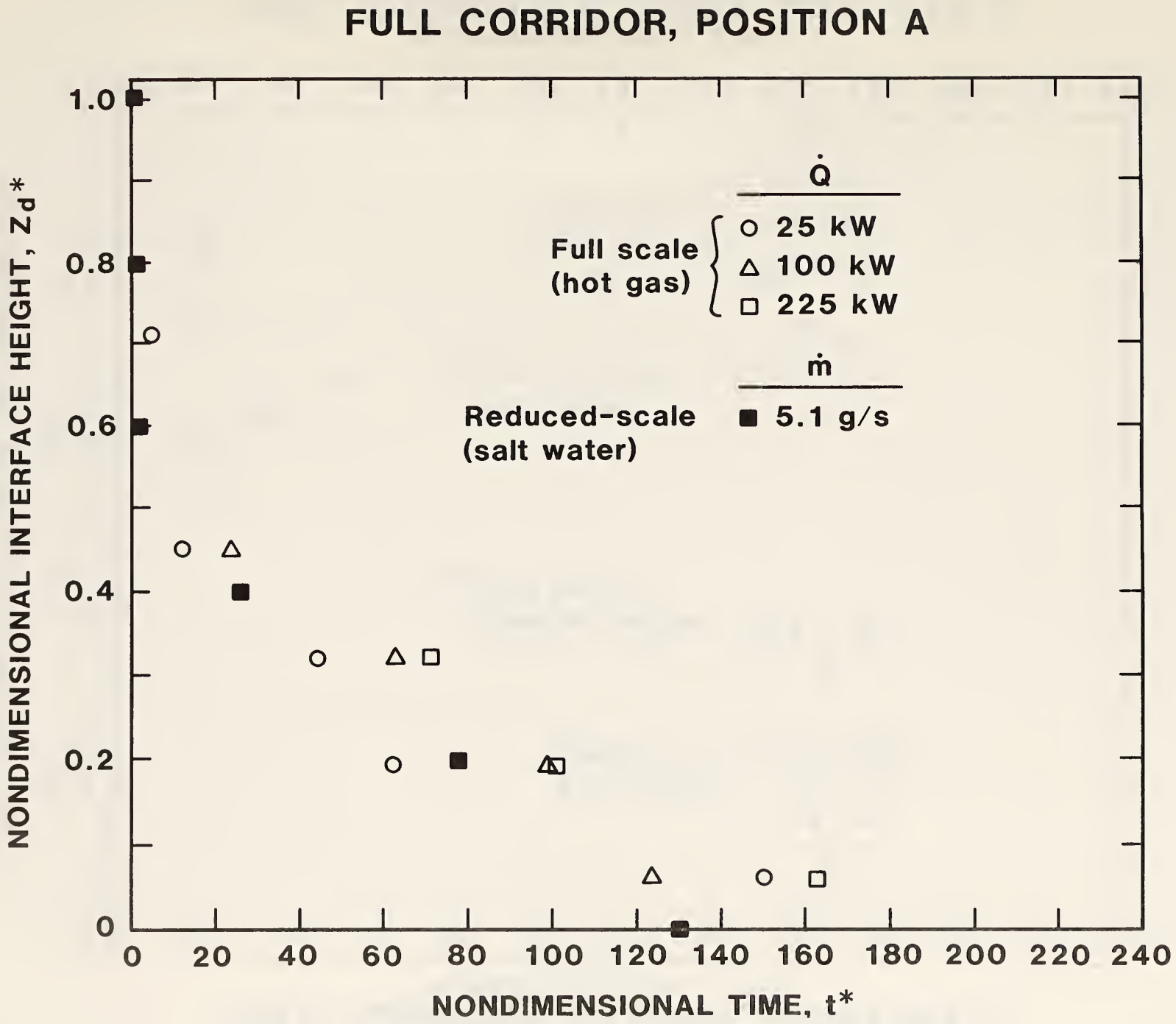


Figure A-6. Results for position D, full corridor configuration.

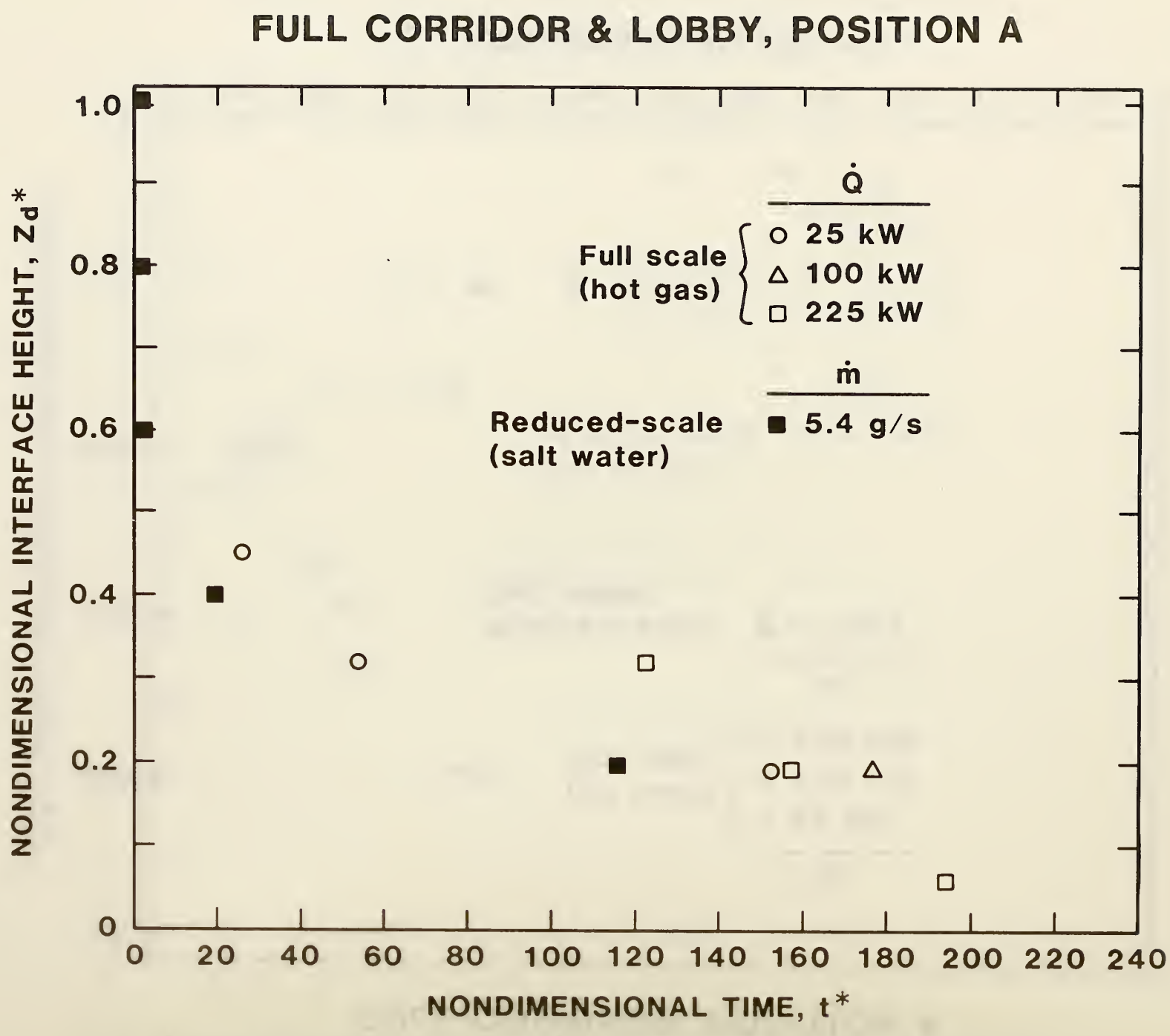


Figure A-7. Results for position A, full corridor plus lobby configuration.

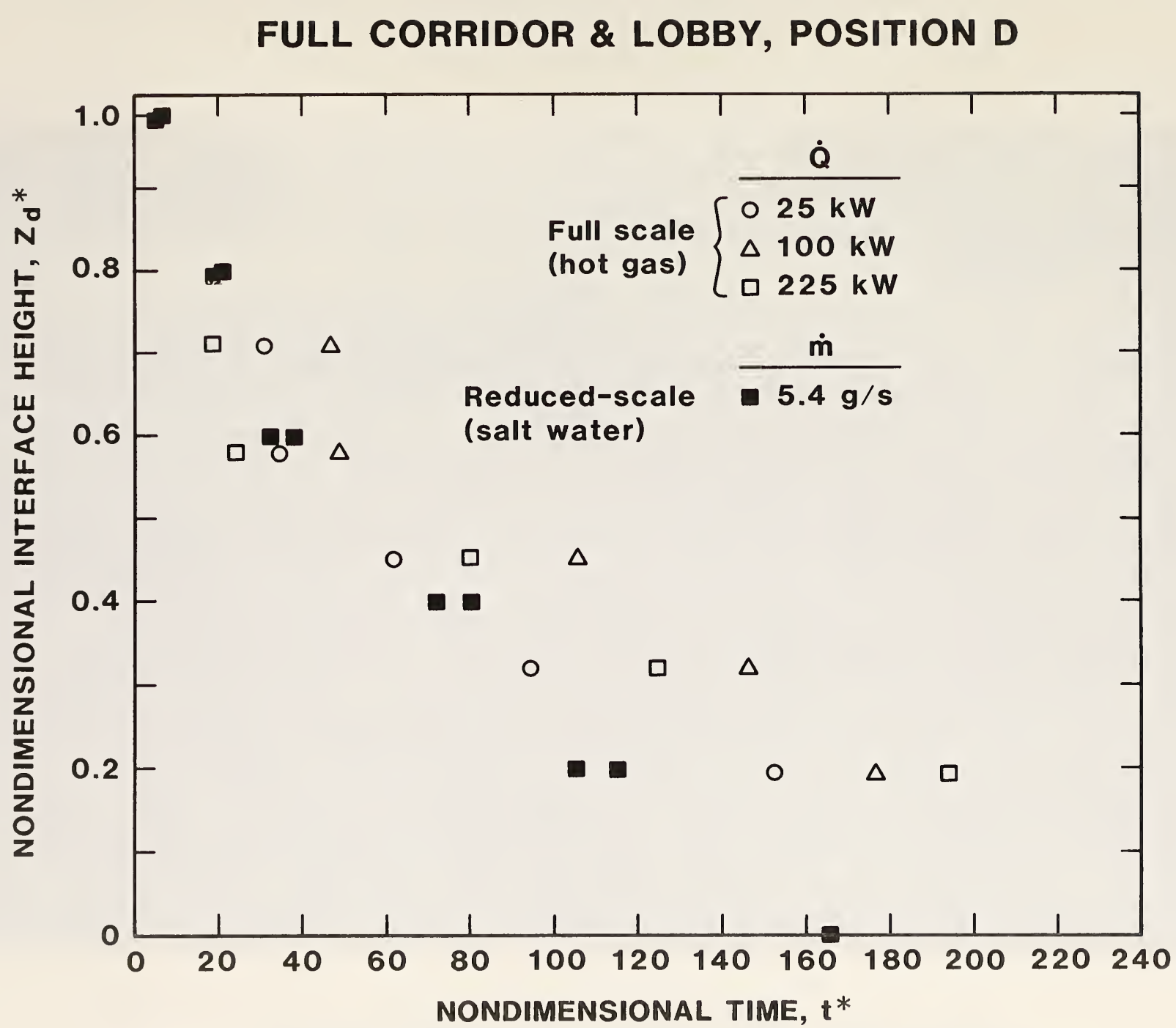


Figure A-8. Results for position D, full corridor plus lobby configuration.

# APPENDIX B

## Photographs of Ship Experiments

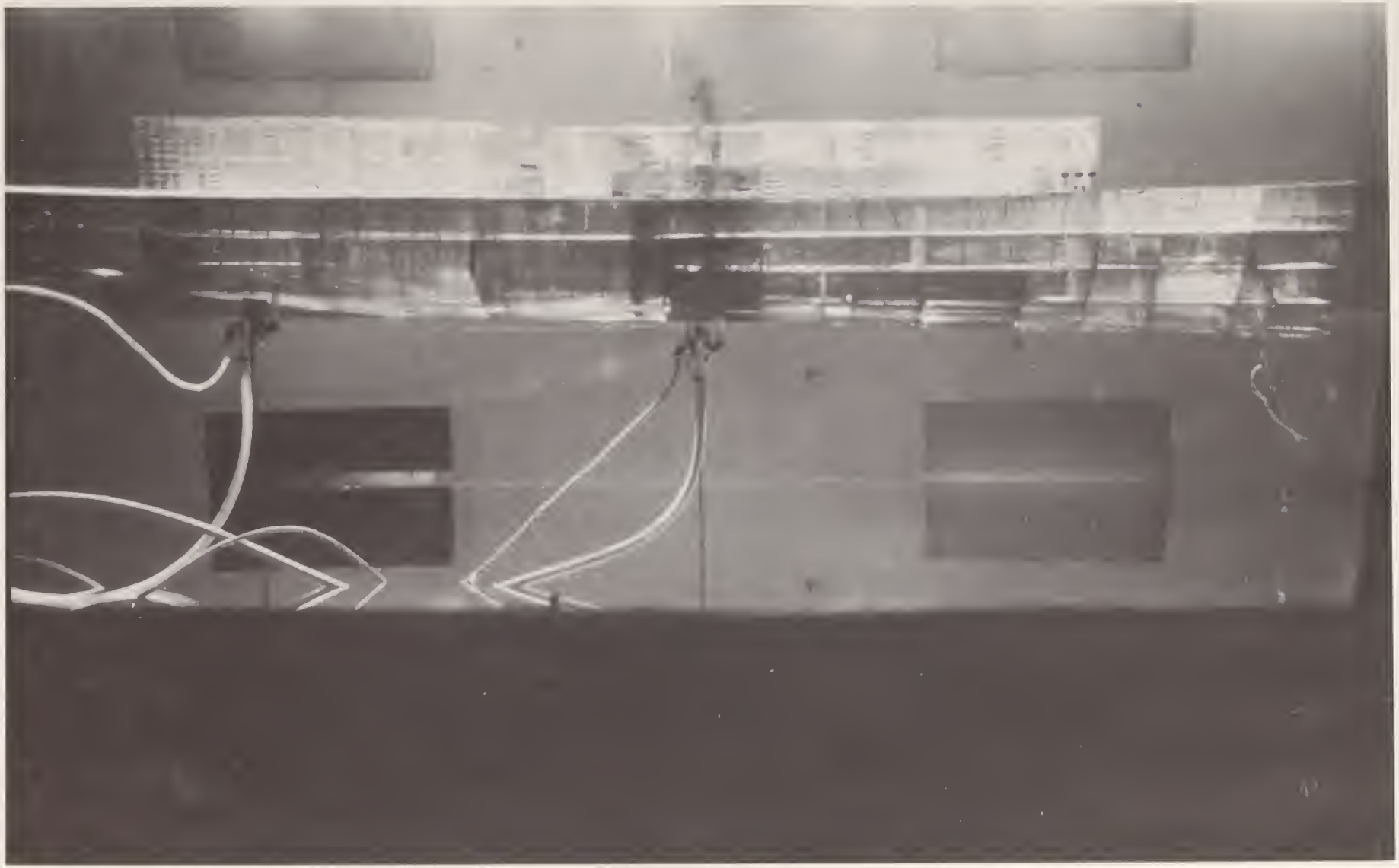

Figure B-1. Inverted photograph of ship experiment approximately 40 s after activation of "225 kW" source in crew quarters. Bow is on right.

Figure B-2. Ship experiment approximately 120 s after activation of "225 kW" source in crew quarters. Bow is to the right.

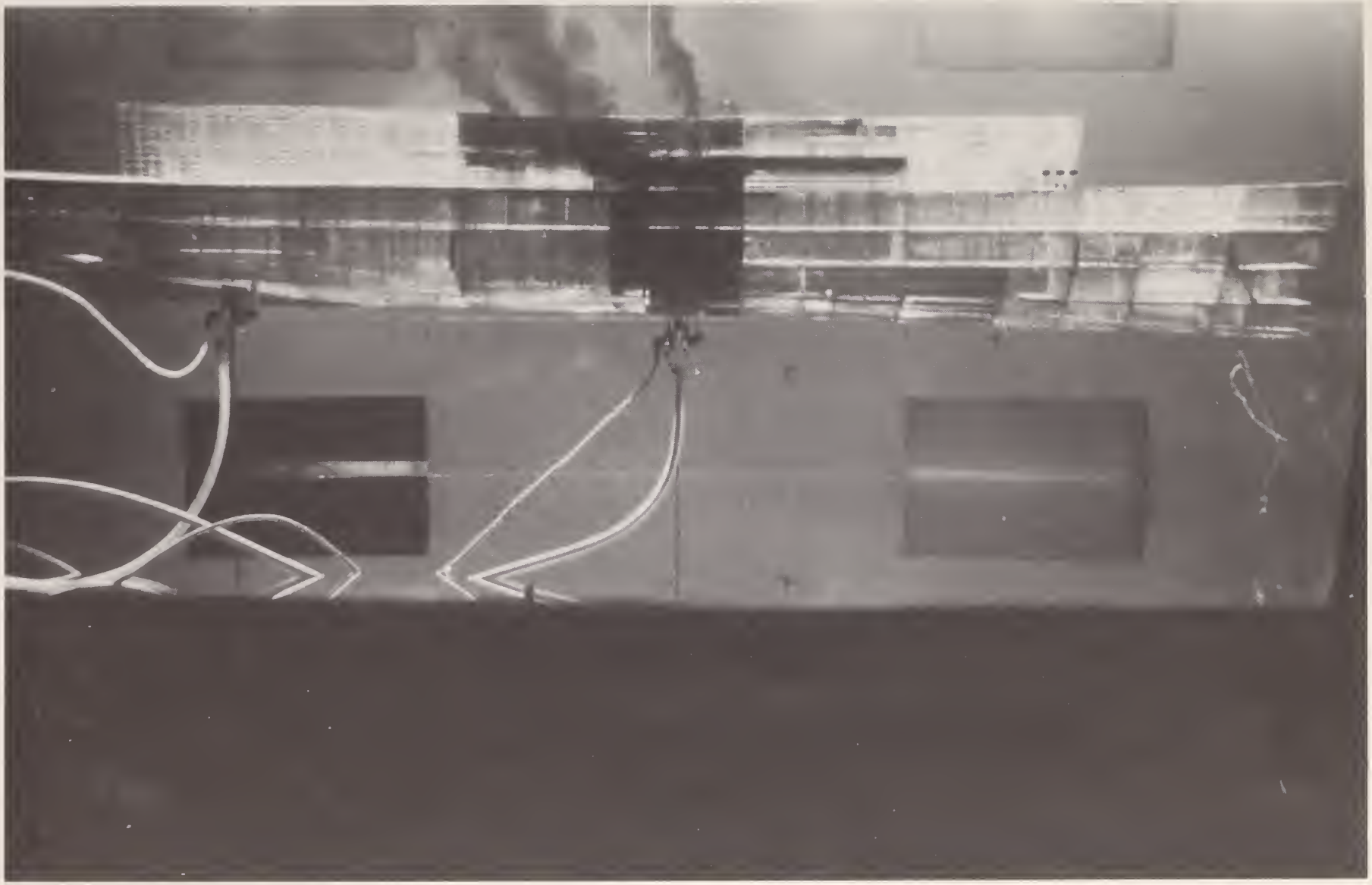

Figure B-3. Ship experiment approximately 240 s after activation of "225 kW" source in crew quarters. Bow is on the right.

Figure B-4. Ship experiment approximately 360 s after activation of "225 kW" source in crew quarters. Bow is to the right.

Figure B-5. Ship experiment a few seconds after activation of source in machinery space. Stern is on the left.

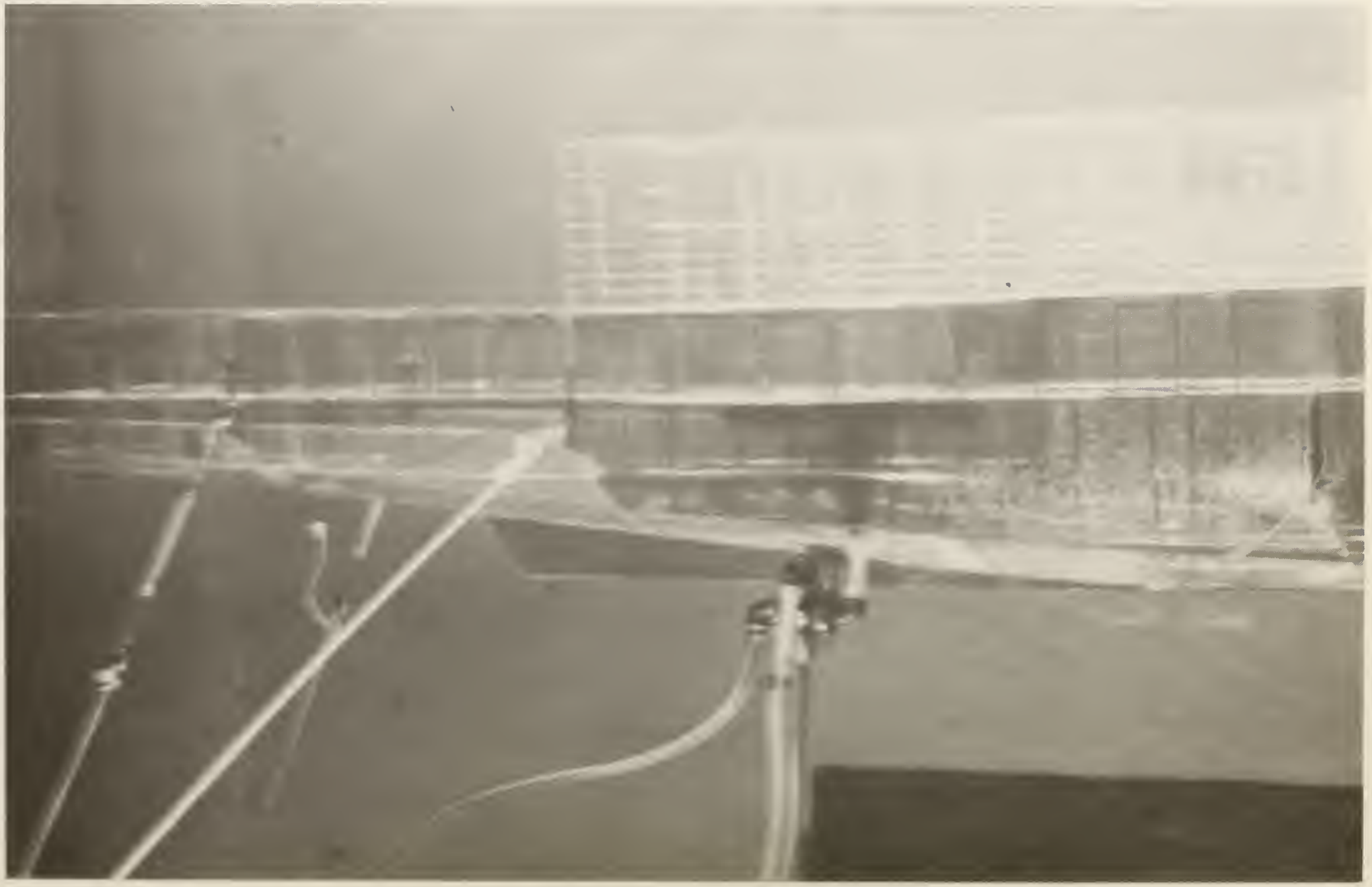

Figure B-6. Ship experiment approximately 8 s after activation of "225 kW" source in machinery space. Stern is on the left.

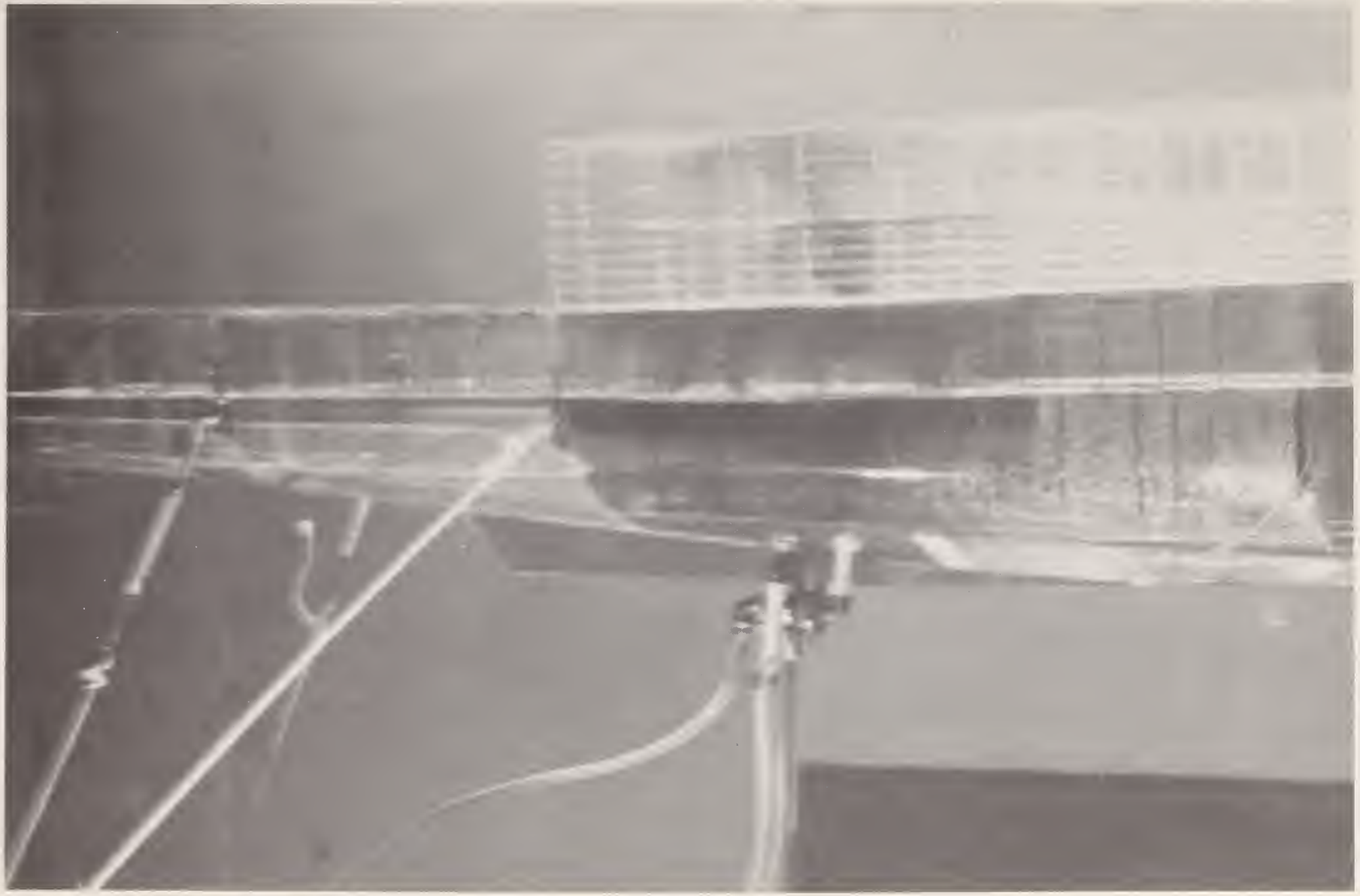

Figure B-7. Ship experiment approximately 40 s after activation of "225 kW" source in machinery space. Salt water flow has entered helicoptor hangers above the main desk. Stern is on the left.

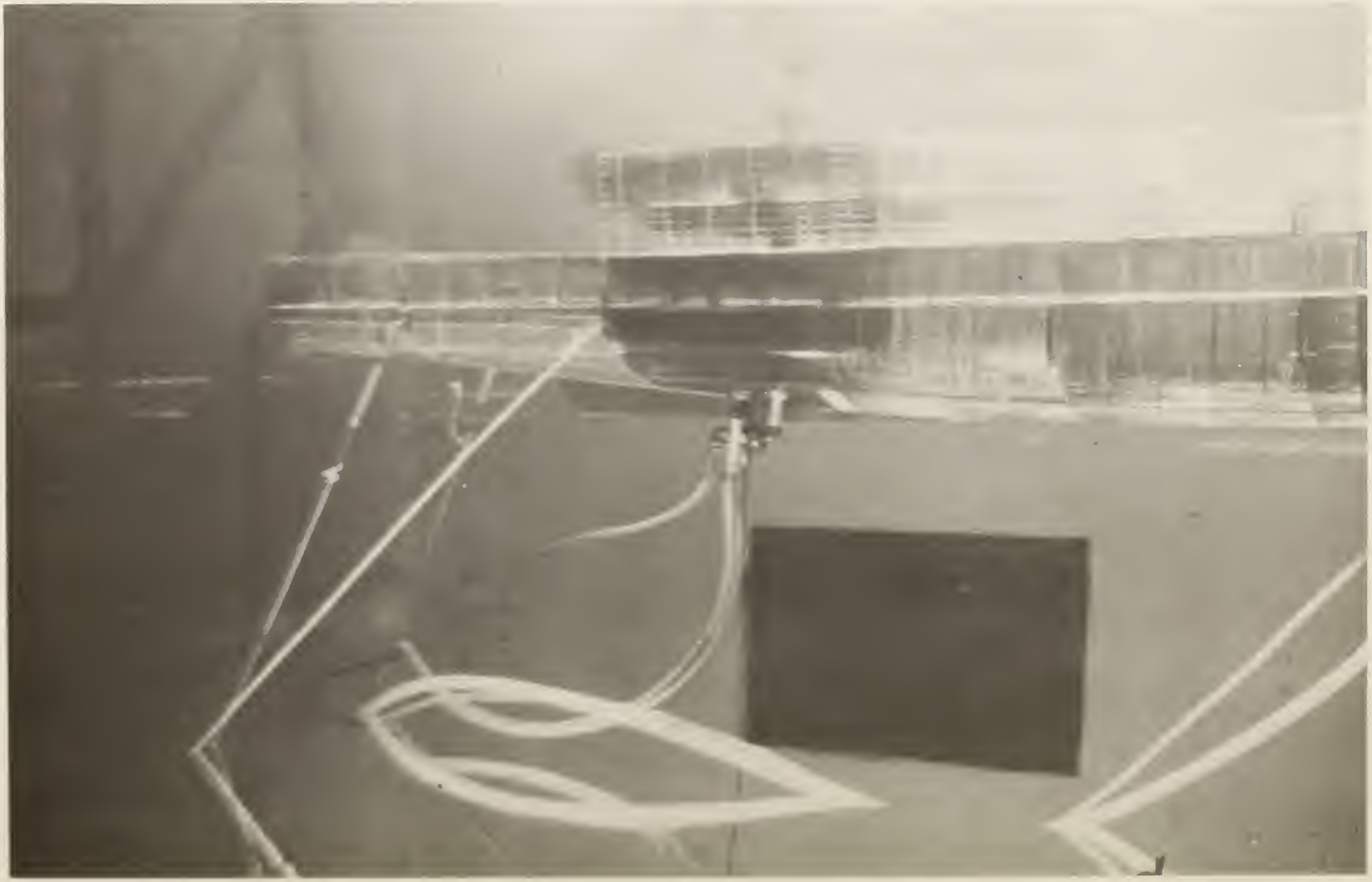

Figure B-8. Ship experiment approximately 70 s after activation of "225 kW" source in machinery space. Salt water flow is just beginning to emerge from helicopter hanger doorways on the left.

Figure B-9. Ship experiment approximately 240 s after activation of "225 kW" source in machinery space.

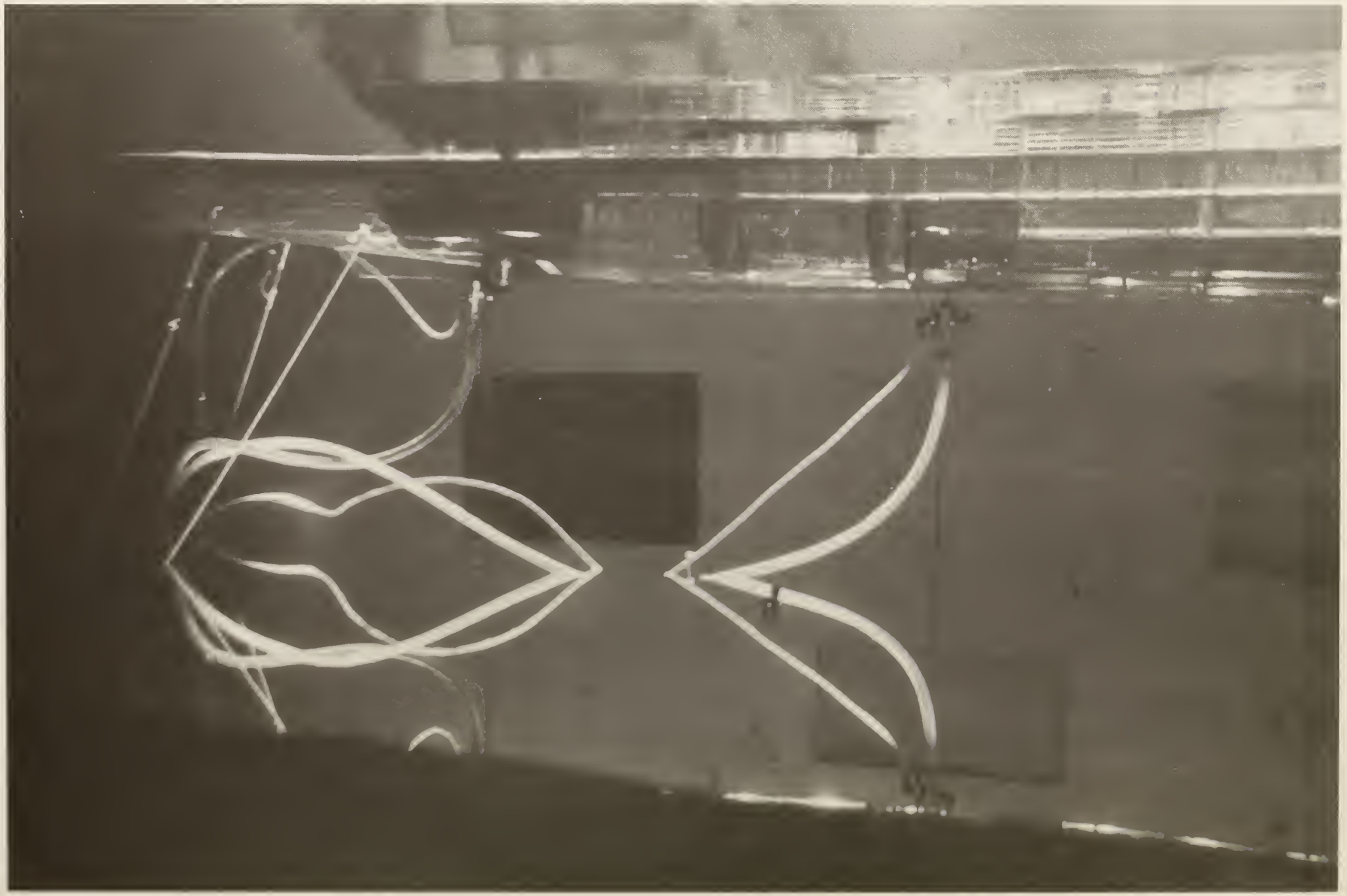

Figure B-10. Ship experiment approximately 300 s after activation of "225 kW" source in machinery space.

NBS-114A (REV. 2-8C)

| U.S. DEPT. OF COMM. BIBLIOGRAPHIC DATA SHEET (See instructions) | 1. PUBLICATION OR REPORT NO. NBSIR-86/3327 | 2. Performing Organ. Report No. | 3. Publication Date March 1986 |
|---|---|---|---|

4. TITLE AND SUBTITLE

Salt Water Modeling of Fire Induced Flows in Multicompartment Enclosures

5. AUTHOR(S)

K.D. Steckler, H.R. Baum, J.G. Quintiere

6. PERFORMING ORGANIZATION (If joint or other than NBS, see instructions)

NATIONAL BUREAU OF STANDARDS
DEPARTMENT OF COMMERCE
WASHINGTON, D.C. 20234
Gaithersburg, MD 20899

7. Contract/Grant No.

8. Type of Report & Period Covered

9. SPONSORING ORGANIZATION NAME AND COMPLETE ADDRESS (Street, City, State, ZIP)

David Taylor Naval Ship Research and Development Center
Bethesda, MD 20084

10. SUPPLEMENTARY NOTES

☐ Document describes a computer program; SF-185, FIPS Software Summary, is attached.

11. ABSTRACT (A 200-word or less factual summary of most significant information. If document includes a significant bibliography or literature survey, mention it here)

Salt water modeling is used to study fire-induced flows in multicompartment structures. Scaling laws relating salt water flows and hot gas flows are developed. Results from 1/20 scale salt water simulations of fire-induced flows in a single-story multiroom structure are shown to be in good agreement with available full-scale results. Experiments involving a 1/20 scale model of a U.S. Navy ship demonstrate the feasibility of using the technique to study hot gas flows in compartmented structures too complex to study economically by other means.

12. KEY WORDS (Six to twelve entries; alphabetical order; capitalize only proper names; and separate key words by semicolons)

buoyant flow; corridors; flow visualization; salt water; scale models; scaling laws; smoke filling; smoke layers

13. AVAILABILITY

☒ Unlimited

☐ For Official Distribution. Do Not Release to NTIS

☐ Order From Superintendent of Documents, U.S. Government Printing Office, Washington, D.C. 20402.

☒ Order From National Technical Information Service (NTIS), Springfield, VA. 22161

14. NO. OF PRINTED PAGES

52

15. Price

$11.95